
BiCompFL: Stochastic Federated Learning with Bi-Directional Compression

Maximilian Egger¹ Rawad Bitar¹ Antonia Wachter-Zeh¹ Nir Weinberger² Deniz Gündüz³

Abstract

We address the prominent communication bottleneck in federated learning (FL). We specifically consider stochastic FL, in which models or compressed model updates are specified by distributions rather than deterministic parameters. Stochastic FL offers a principled approach to compression, and has been shown to reduce the communication load under perfect downlink transmission from the federator to the clients. However, in practice, both the uplink and downlink communications are constrained. We show that bi-directional compression for stochastic FL has inherent challenges, which we address by introducing BiCOMPFL. Our BiCOMPFL is experimentally shown to reduce the communication cost by an order of magnitude compared to multiple benchmarks, while maintaining state-of-the-art accuracies. Theoretically, we study the communication cost of BiCOMPFL through a new analysis of an importance-sampling based technique, which exposes the interplay between uplink and downlink communication costs.

1 Introduction

Federated learning (FL) is a widely used and well-studied machine learning (ML) framework, where multiple clients orchestrated by a federator collaborate to train an ML model (McMahan et al., 2017). Communication efficiency, privacy, security, and data heterogeneity are critical challenges in FL that have been extensively studied (Zhang et al., 2021; Wen et al., 2023). In principle, FL is a *bi-directional* process, and with the increasing size of ML models, massive amounts of data are communicated be-

tween the federator and the clients. Reducing *uplink* communication from clients to the federator has been the focus of many studies, mainly within the framework of lossy gradient compression, e.g., (Seide et al., 2014; Alistarh et al., 2017; Isik et al., 2024). However, reducing the cost of *downlink* transmission to communicate the updated global model from the federator to the clients has received relatively less attention, although it is as costly and can be a major bottleneck when training over a wireless network. An ongoing body of research aims to study the communication bottleneck in downlink transmission, by combining tools from gradient compression, momentum, and error-feedback (Stich et al., 2018; Tang et al., 2019; Xie et al., 2020; Amiri et al., 2020; Philippenko & Dieuleveut, 2020; Gruntkowska et al., 2023; Tyurin & Richtárik, 2023; Dorfman et al., 2023; Gruntkowska et al., 2024). All these works are focused on non-stochastic (or non-Bayesian) settings. However, the state-of-the-art performance under limited uplink communication is achieved by stochastic compression methods, such as QSGD (Alistarh et al., 2017), QLSD (Vono et al., 2022), dithered quantization (Abdi & Fekri, 2019) and FedPM (Isik et al., 2023), in which the clients send samples from a local distribution, and the federator estimates the mean of the clients’ distributions by averaging these samples. To address this gap, in this work, we study the performance of stochastic FL with limited communication in both directions, and propose a method that obtains state-of-the-art results. Moreover, we show that our method can actually reduce the communication cost even in conventional FL with stochastic compression.

A fundamental approach to both uni-directional and bi-directional compression schemes involves quantizing transmitted update vectors to finite resolutions. The trade-off between communication cost (or compression) and the quantization distortion has been extensively studied under the framework of rate-distortion theory (Cover & Thomas, 2006). However, classical rate-distortion is not well suited for analyzing how quantization affects the convergence of stochastic gradient-based optimization, as they rely on the joint compression of many samples and assume additive distortion measures. Consequently, it becomes difficult to characterize the fundamental trade-off between the communication cost and the convergence rates.

An alternative stochastic FL approach was proposed by

This project has received funding from the German Research Foundation (DFG) under Grant Agreement Nos. BI 2492/1-1 and WA 3907/7-1, and from UKRI for project AI-R (ERC-Consolidator Grant, EP/X030806/1). The work of N.W. was partly supported by the Israel Science Foundation (ISF), grant no. 1782/22. ¹Technical University of Munich ²Israel Institute of Technology ³Imperial College London. Correspondence to: Maximilian Egger <maximilian.egger@tum.de>.

Isik et al. (2024), which applies to a variety of Bayesian FL solutions as well as to standard gradient-based methods with stochastic compression. Communication reduction is achieved by *minimal random coding* (MRC), which allows the federator to directly sample from the updated local distributions, rather than obtaining quantized versions of samples locally generated by each of the clients. This enables a direct evaluation of the communication cost when a shared common prior distribution, referred to as *side information*, and sufficient common randomness are available between the federator and the clients. When the downlink communication is unlimited, the global model distribution at the federator can then be shared with all the clients, and serves as a natural side information, i.e., common prior. However, this is impossible under downlink communication constraints. This necessitates developing new algorithms and analysis, as we carry in this paper.

The core research question we address is: *Can joint uplink and downlink compression reduce communication bottlenecks in stochastic FL?* We answer this question in the affirmative, and we develop and analyze stochastic FL algorithms with bi-directional compression. We utilize MRC with appropriate priors, and accurately characterize the uplink and downlink communication costs and the compression error. When applied to conventional gradient-based methods, we prove a contraction property of our compression method, thereby facilitating convergence analysis for both uni- and bi-directional MRC-based stochastic compression. We also examine key performance factors including client data heterogeneity, availability of shared randomness among clients, and various hyperparameters. Our main contributions are summarized next.

1.1 Contributions

- We propose two algorithms for bi-directional stochastic FL based on the availability of shared randomness: one for the case when globally shared randomness is available, and another for the case when only private shared randomness between each client and the federator is available. Both algorithms use carefully chosen side information to transmit samples from the desired distribution through MRC.
- We experimentally validate our method on existing baselines, and demonstrate *order-wise* reductions in the communication cost, while maintaining similar accuracies. We thoroughly investigate the role of shared randomness and the choice of side information.
- We apply our method to stochastic compression in conventional FL, achieving substantial reductions in communication cost. We establish convergence guarantees by proving a contraction property for the biased compressors used in our algorithms.

- We develop a theoretical framework for MRC to quantify communication costs in stochastic FL with bi-directional compression. Our findings go beyond the established analysis of Chatterjee & Diaconis (2018), providing refined results for Bernoulli distributions that may be of independent interest. Our theoretical framework further allows targeted convergence analysis, and provides techniques applicable to other distributions.

2 Preliminaries: Stochastic FL with Bi-Directional Compression

We propose a general stochastic FL algorithm that employs stochastic bi-directional compression based on MRC. In what follows, we shortly review these concepts.

Stochastic FL. A set of n clients collaboratively and iteratively train a model, e.g., a neural network, under the orchestration of a federator. Client $i \in [n] := \{1, \dots, n\}$ possesses a dataset \mathcal{D}_i . We differentiate between homogeneous data, where \mathcal{D}_i is drawn independently from the same distribution for all clients (i.i.d.), and heterogeneous data, where each \mathcal{D}_i may come from a different distribution (non i.i.d.). At each iteration t of the training, the federator holds a model θ_t described by a probability distribution. After downlink transmission, each client i has an estimate $\hat{\theta}_{i,t}$ of θ_t , and locally optimizes $\hat{\theta}_{i,t}$ to obtain a local probabilistic model called *posterior* q_i^t . Compressed versions of the clients' posteriors q_i^t are transmitted back to the federator on the uplink to obtain an estimate \hat{q}_i^t . The federator aggregates the received posteriors using an aggregation rule $R(\cdot)$ to obtain a refined global probability distribution $\theta_{t+1} = R(\{\hat{q}_i^t\}_{i \in [n]})$. A simple aggregation rule $R(\cdot)$ is the average over all clients' posteriors. This process is repeated until a certain convergence criterion is met. In many stochastic FL settings, the transmitted client updates \hat{q}_i^t are samples from the posterior distribution q_i^t .

Furthermore, our definition of Stochastic FL encompasses conventional FL with stochastic quantization. The same procedure as above follows with those differences: (i) the federator holds a model θ_t with deterministic parameters; (ii) each client i locally optimizes $\hat{\theta}_{i,t}$ to obtain a local gradient g_i^t . A stochastic compression $Q_s(\cdot)$ is applied on the client's gradient to obtain a posterior distribution q_i^t from $Q_s(g_i^t)$; (iii) samples of q_i^t are transmitted to the federator on the uplink to obtain an estimate of the gradient, which we still denote by \hat{q}_i^t ; and (iv) the federator updates the global model as $\theta_{t+1} = \theta_t - \eta R(\{\hat{q}_i^t\}_{i \in [n]})$, with learning rate η . We will investigate both settings, with a prominent focus on the former.

Stochastic Compression by MRC. To efficiently transmit samples from the posterior q_i^t , we employ MRC (Havasi et al., 2019) to leverage common side information present at the federator and the clients, and shared random-

ness. This method serves as stochastic compressor $\mathcal{C}_{\text{mrc}}(\cdot)$, which takes as input a posterior distribution Q and a prior distribution P , and outputs a sample from a distribution \hat{Q} close to Q . In MRC, the encoder and decoder generate n_{IS} samples $\{X_i\}_{i \in [n_{\text{IS}}]}$ from P . The encoder computes a categorical distribution W , with $W(i) = \frac{Q(X_i)/P(X_i)}{\sum_{i=1}^{n_{\text{IS}}} Q(X_i)/P(X_i)}$, and transmits an index $i \sim W$ with $\log_2(n_{\text{IS}})$ bits. The encoder sets $n_{\text{IS}} = \Theta(\exp(\text{D}_{\text{KL}}(Q\|P)))$, where $\text{D}_{\text{KL}}(Q\|P)$ denotes the KL-divergence between Q and P (Chatterjee & Diaconis, 2018; Havasi et al., 2019). For two Bernoulli distributions with parameters q and p we use the short notations $\text{d}_{\text{KL}}(q\|p)$ and $\mathcal{C}_{\text{mrc}}(q, p)$.

3 BiCompFL

In this section, we introduce our proposed scheme, BiCompFL, a bi-directional stochastic compression strategy that uses MRC to reduce both uplink and downlink communication costs. The scheme relies on the availability of shared randomness between each of the clients and the federator, which can be implemented using pseudo-random sequences generated from a common seed. We distinguish between two types of shared randomness: private shared randomness (between individual clients and the federator) and global shared common randomness (among all parties), with the latter being more challenging to implement in practice. We assume all clients and the federator share the same global model $\hat{\theta}_0$ at initialization. This does not incur any communication cost when global shared randomness is available, but necessitates an initial model transmission from the federator to clients when only private shared randomness exists.

BiCompFL: The General Algorithm. Our method serves as a general framework for stochastic optimization procedures. We explain BiCompFL for Bayesian FL and show in the sequel how it can be used for conventional FL with stochastic quantization. Consider probabilistic mask training (similar to FedPM, (Isik et al., 2023)) as an example of Bayesian FL. Let $[0, 1] := \{x \in \mathbb{R} : 0 \leq x \leq 1\}$. The models $\theta_t \in [0, 1]^d$ of dimension d are parameters of Bernoulli distributions. Those parameters determine for each weight of a randomly initialized network with fixed weights w whether it is activated or not. During inference, the weights w are masked with samples $x^t \in \{0, 1\}^d \sim \theta_t$, i.e., the network weights are $w \odot x^t$. We start with a general description, which is valid for the cases of global and private shared randomness.

At iteration $t = 0$, each client $i \in [n]$ shares with the federator the same global model, i.e., $\hat{\theta}_{i,0} = \theta_0$, for all $i \in [n]$. At iteration t , each client i locally trains model $\hat{\theta}_{i,t}$ in L local iterations. In our previous example, when training Bernoulli distributions to mask a random network, the pa-

rameters are mapped to scores in a dual space, which are then trained for L local iterations $m \in [L]$ using stochastic gradient descent. Mapping the trained scores back to the primal space, each client i obtains a model update in terms of a posterior q_i^t . We refer to Appendix G for details. This optimization principle is a special instance of mirror descent, which, in the special case of optimizing over Bernoulli distributions, leads to a point-wise minimization with respect to a KL-proximity term (as opposed to the Euclidean distance in standard SGD, cf. Appendix D for details). The KL-divergence between the updated local model and the global model directly determines the communication cost. Hence, we *regularize* the minimization of the loss function by the communication cost. This property renders our method superior to various baselines.

To convey the model update q_i^t to the federator, each client employs $\mathcal{C}_{\text{mrc}}(\cdot)$ in B blocks of size d/B each (assuming $B|d$) with a prior distribution $p_{i,u}^t$, which is set to $p_{i,u}^0 = \hat{\theta}_{i,0}$ at iteration $t = 0$. The choice of $p_{i,u}^t$ for $t > 0$ will be clarified later. For each block $b \in [d/B]$, client i conveys n_{UL} samples $\{y_{i,\ell}^t\}_{\ell \in [n_{\text{UL}}]}$ of q_i^t to the federator by transmitting for each block b an index $I_{i,\ell}^b$ with $\log_2(n_{\text{IS}})$ bits, where n_{IS} is the number of samples per block, generated from the prior distribution $p_{i,u}^t$ at both the client and the federator using the available shared randomness. The samples of all blocks are concatenated for each ℓ . Hence, the federator obtains an estimate of client i 's posterior distribution using the empirical average $\hat{q}_i^t = \frac{1}{n_{\text{UL}}} \sum_{\ell=1}^{n_{\text{UL}}} y_{i,\ell}^t$.

By averaging the estimates \hat{q}_i^t for all the clients' models, the federator updates the global model as $\theta_{t+1} = \frac{1}{n} \sum_{i=1}^n \hat{q}_i^t$. To transmit the new model to each client i , we assume the existence of a common prior $p_{i,d}^t$ shared by the federator and the clients. With $p_{i,d}^t$, the federator performs MRC in B blocks of size d/B to make client i sample from, and thereby estimate, the latest global model θ_{t+1} . The client samples n_{DL} masks $\{x_{i,\ell}^t\}_{\ell \in [n_{\text{DL}}]}$, each incurring a communication cost of $B \log_2(n_{\text{IS}})$ bits. An estimate of the updated global model is obtained by concatenating the reconstructed samples for all the blocks $b \in [B]$, and averaging over all masks $\hat{\theta}_{i,t+1} = \frac{1}{n_{\text{DL}}} \sum_{\ell=1}^{n_{\text{DL}}} x_{i,\ell}^t$.

Since the number of clients is typically large, it often suffices to choose $n_{\text{UL}} = 1$. The clients' contributions are averaged at the federator, effectively reducing the noise due to the MRC step. This allowed Isik et al. (2024) to theoretically analyze the uplink communication cost for importance sampling-based stochastic communication of model updates. We will follow a similar approach for downlink communication; however, since downlink communication cannot benefit from the averaging effect of multiple clients, we reduce the variance of the model estimate in the downlink by setting $n_{\text{DL}} = n \cdot n_{\text{UL}}$.

Algorithm 1 BiCOMPFL-GR with Global Randomness

Require: Both clients and federator initialize the same global model θ_0 using a shared seed

Ensure: Clients set prior $p^t = \hat{\theta}_{i,0} = \theta_0, \forall i \in [n]$

```

1: repeat
2:   for Client  $i \in [n]$  do
3:      $q_i^t \leftarrow$  Local training of  $\hat{\theta}_{i,t}$ 
4:     Sample indices  $I_{i,\ell}^b, \ell \in [n_{UL}], b \in [B]$  from  $q_i^t$  with
       prior  $p^t$  and transmit to federator to reconstruct  $\hat{q}_i^t$ 
5:   end for
6:   Federator updates global model  $\theta_{t+1} = \frac{1}{n} \sum_{i=1}^n \hat{q}_i^t$ 
7:   Federator relays to client  $j$  the other clients' indices
        $\{I_{i,\ell}^b\}_{\ell \in [n_{UL}], b \in [B], i \in [n] \setminus \{j\}}$ 
8:   for Clients  $i \in [n]$  do
9:     Reconstruct  $\hat{\theta}_{i,t+1} = \frac{1}{n} \sum_{i=1}^n \hat{q}_i^t$  from  $\{I_{i,\ell}^b\}$ 
10:  end for
11:  Clients and federator set prior  $p^t = \hat{\theta}_{t+1}$ 
12:   $t \leftarrow t + 1$ 
13: until Convergence
    
```

The choice of the priors $p_{i,u}^t$ and $p_{i,d}^t$ for MRC in the uplink and downlink channels, respectively, crucially affects the performance and the communication cost of the algorithm. As a first-order characterization, the communication cost of MRC is determined by $D_{\text{KL}}(q_i^t \| p_{i,u}^t)$ in the uplink and by $D_{\text{KL}}(\theta_{t+1} \| p_{i,d}^t)$ in the downlink.

Global Randomness. When global shared randomness is available, all clients can maintain the same priors at each iteration t , and, thereby, obtain the same global model estimates $\hat{\theta}_{i,t}$. The global model is known to the clients and the federator from initialization, and synchronization among all clients is ensured by choosing as prior $p_{i,u}^t = p_{i,d}^t$ the latest estimate of the global model $\hat{\theta}_{i,t}$. The clients utilize the globally shared randomness to sample the exact same samples from the same prior for uplink transmission at all iterations. Selected indices of such samples are transmitted to the federator to convey an estimate \hat{q}_i^t of the posterior q_i^t , who reconstructs the global model θ_{t+1} . Using the same prior in the downlink, i.e., the global model from the previous iteration, the updated model can be transmitted to the clients through MRC. Leveraging the shared randomness, all clients $i \in [n]$ sample from the same prior, and thus obtain the exact same estimate of the global model $\hat{\theta}_{i,t+1} = \hat{\theta}_{t+1}$, for all $i \in [n]$. Hence, we have that $p_{i,u}^t = p_{i,d}^t = \hat{\theta}_t$ for all $i \in [n]$.

In this version, the federator reconstructs the global model from estimates of the client posteriors \hat{q}_i^t . However, in the uplink, all clients sample from the same prior, which enables further improvements. Naively, the federator will reconstruct the global model using the indices $I_{i,\ell}^b$ for $b \in [B], \ell \in [n_{UL}]$ received by the clients $i \in [n]$ through MRC, followed by an additional round of MRC for downlink

Algorithm 2 BiCOMPFL-PR with Private Randomness

Require: Both clients and federator initialize the same global model θ_0 using a shared seed

Ensure: Clients set prior $p_{i,u}^t = p_{i,d}^t = \hat{\theta}_{i,0} = \theta_0, \forall i \in [n]$

```

1: repeat
2:   for Client  $i \in [n]$  do
3:      $q_i^t \leftarrow$  Local training of  $\hat{\theta}_{i,t}$ 
4:     Federator employs  $\mathcal{C}_{\text{mrc}}(q_i^t, p_{i,u}^t)$  to draw  $n_{UL}$  sam-
       ples  $y_{i,\ell}^t \sim q_i^t$  using prior  $p_{i,u}^t$ 
5:     Federator est. client's posterior  $\hat{q}_i^t = \frac{1}{n_{UL}} \sum_{\ell=1}^{n_{UL}} y_{i,\ell}^t$ 
6:   end for
7:   Federator updates global model  $\theta_{t+1} = \frac{1}{n} \sum_{i=1}^n \hat{q}_i^t$ 
8:   for Clients  $i \in [n]$  do
9:     Client employs  $\mathcal{C}_{\text{mrc}}(\theta_{t+1}, p_{i,d}^t)$  to draw  $n_{DL}$  samples
        $x_{i,\ell}^t \sim \theta_{t+1}$  using prior  $p_{i,d}^t$ 
10:    Client est. global model:  $\hat{\theta}_{i,t+1} = \frac{1}{n_{DL}} \sum_{\ell=1}^{n_{DL}} x_{i,\ell}^t$ 
11:    Clients set prior  $p_{i,u}^t = p_{i,d}^t = \hat{\theta}_{i,t+1}$ 
12:  end for
13:   $t \leftarrow t + 1$ 
14: until Convergence
    
```

transmission. Instead, and more efficiently, the federator can simply relay the indices to the respective other clients (i.e., client j receives $I_{i,\ell}^b$ for $b \in [B], i \in [n] \setminus \{j\}, \ell \in [n_{UL}]$), which reconstruct the same updated global model individually. This avoids introducing additional noise by a second round of compression and allows better convergence without additional communication facilitated by global randomness. We term this approach BiCOMPFL-GR and summarize the procedure in Algorithm 1.

Private Randomness. Without global randomness, maintaining the same prior among all clients is impossible without introducing additional communication. Instead, an additional round of MRC is needed for the downlink transmission, and each client obtains a different estimate of the global model $\hat{\theta}_{i,t}$ at each iteration. Hence, the clients' local trainings start from different estimates of the global model. In a non-stochastic setting, such a phenomenon has only been considered by Philippenko & Dieuleveut (2021); Gruntkowska et al. (2024). This raises the questions of the additional cost incurred due to lack of shared randomness in terms of both the convergence speed and the communication load and the choice of the priors $p_{i,u}^t$ and $p_{i,d}^t$.

For the uplink transmission of client i , any convex combination of $\hat{\theta}_{i,t}$ and \hat{q}_i^t can be used as prior, i.e., $p_{i,u}^t = \lambda \hat{\theta}_{i,t} + (1 - \lambda) \hat{q}_i^t$, for some $0 \leq \lambda \leq 1$.¹ This is due to the availability of both quantities at the federator and client i . However, small λ values are not expected to reduce the cost of communication reflected by $d_{\text{KL}}(q_i^t \| p_{i,u}^t)$

¹This adds a negligible cost of transmitting λ if it is to be optimized at each round, cf. Appendix J.2 for details.

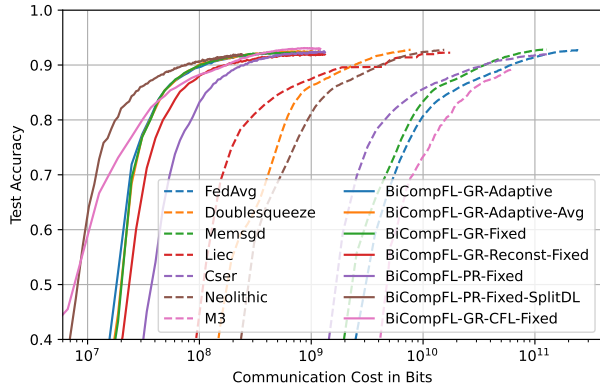


Figure 1: Test accuracy for BiCOMPFL and baselines on Fashion MNIST 4CNN on i.i.d. data.

since the previous global model estimate is likely to be similarly different from the posterior (in terms of the KL-divergence) than the previous posterior estimate of the federator. Indeed, our numerical experiments have shown that the savings from choosing $\lambda \neq 1$, i.e., priors other than $\hat{\theta}_{i,t}$, are not significant. For simplicity, we thus propose to use $p_{i,u}^t = p_{i,d}^t = \hat{\theta}_{i,t}$. We term this approach BiCOMPFL-PR and summarize the procedure in Algorithm 2. Choosing different priors is possible and only affects line 11 in Algorithm 2. We mention in passing that BiCOMPFL-PR allows partial client participation, which is incompatible with shared randomness and the method BiCOMPFL-GR.

Block Allocation. We consider three different block allocation strategies: 1) fixed block size (referred to as “Fixed” in the experiments), where each block $b \in [B]$ is of the same size and constant across all t ; 2) adaptive block allocation (Adaptive) as proposed by Isik et al. (2024), where each block size is separately optimized each iteration t ; and 3) adaptive average allocation (Adaptive-Avg), where the block sizes are equal but optimized at each iteration t according to the average KL-divergence per block. We refer the reader to Appendix E for a detailed discussion on this.

4 Experiments

We conduct experiments to evaluate the performance of our proposed BiCOMPFL-GR and BiCOMPFL-PR schemes, and compare against baseline FL strategies without compression (FedAvg or PSGD) (McMahan et al., 2017) and several non-stochastic bi-directional compression schemes that employ different combinations of compression, error-feedback, and momentum. In particular, we compare against DOUBLEQUEUE (Tang et al., 2019), MEM-SGD (Stich et al., 2018), NEOLITHIC (Huang et al., 2022), CSER (Xie et al., 2020), and the recently proposed LIEC (Cheng et al., 2024). SignSGD (Seide et al., 2014) serves to compress the transmitted gradients for all the schemes. We fur-

ther compare with M3 (Gruntkowska et al., 2024), which partitions the model into disjoint parts for downlink transmission and transmits to each client a different part of the model. While M3 is focused on RandK compression for the uplink (i.e., transmitting random K entries of the gradient), we use TopK (Wangni et al., 2018; Shi et al., 2019), which we found to achieve much more stable results.

As mentioned above, the mirror descent approach outlined in Section 3 inherently minimizes the communication cost as a by-product; and hence, provides a strong candidate for communication-efficient stochastic FL. Nonetheless, we show how our method can be used to improve the communication efficiency in conventional FL by using the uplink and downlink compression $\mathcal{C}_{\text{mrc}}(\cdot)$ combined with stochastic quantizers, e.g., (Alistarh et al., 2017). In Section 5, we pave the way to convergence guarantees by proving a contraction property of $\mathcal{C}_{\text{mrc}}(\cdot)$ composed with a stochastic quantization $Q_s(\cdot)$ of gradients g_i^t . To compare our method to the baselines that use SignSGD as compressor, we evaluate BiCOMPFL-GR in a conventional federated learning (CFL) task with a stochastic variant of SignSGD. We replace the mirror descent over Bernoulli masks by a standard learning procedure over a deterministic model, which takes as input the global model estimate $\hat{\theta}_{i,t}$, computes a gradient g_i^t (over L local epochs), and outputs a distribution $Q_s(g_i^t)$. In stochastic SignSGD, $Q_s(\cdot)$ transforms each gradient entry $g_{i,e}^t$ to a Bernoulli random variable with parameter $q_{i,e}^t = 1/(1 + \exp(-g_{i,e}^t/K))$ for some $K > 0$, where the random variable takes value $+1$ with probability $q_{i,e}^t$, and -1 otherwise. We then employ $\mathcal{C}_{\text{mrc}}(q_i^t, p_{i,u}^t)$ to obtain samples $y_{i,\ell}^t$, where the compression is performed element-wise. We apply this method to BiCOMPFL-GR where Step 6 is replaced by $\theta_{t+1} = \theta_t - \eta_s \frac{1}{n} \sum_{i=1}^n \hat{q}_i^t$, where $\hat{q}_i^t = \frac{1}{n_{\text{UL}}} \sum_{\ell=1}^{n_{\text{UL}}} y_{i,\ell}^t$ and η_s is the federator’s learning rate. Step 9 is modified accordingly. The priors p^t are chosen to be Bernoulli random variables with parameter 0.5. We will refer to this method as BiCOMPFL-GR-CFL.

We study the setting of $n = 10$ clients collaboratively training a convolutional neural network (CNN)-based classifier for the datasets MNIST, Fashion-MNIST and CIFAR-10 under the orchestration of a federator. For MNIST, we use two different models, LeNet-5 (Lecun et al., 1998) and a 4-layer convolutional neural network (4CNN) proposed by Ramanujan et al. (2020). The latter is also used to train on Fashion MNIST. For CIFAR-10, we use a larger neural network with 6 convolutional layers (6CNN). We train MNIST and Fashion-MNIST for 200 global iterations and CIFAR-10 for 400 global iterations. Through all experiments and datasets, we carry $L = 3$ local iterations per client per global iteration. We evaluate the performance of the schemes in two different settings: with uniform data allocation (i.i.d.) to model homogeneous systems and a

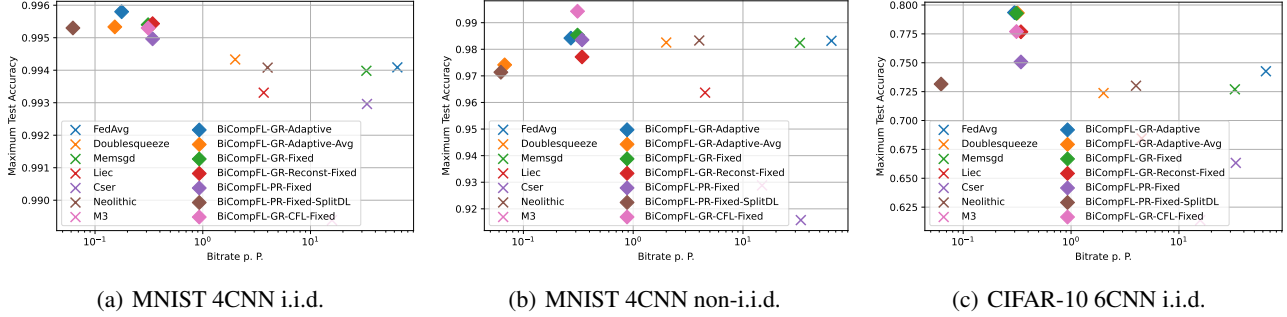


Figure 2: Maximum test accuracy as a function of the total communication cost measured as the bitrate per parameter.

non-i.i.d. setting to model heterogeneous systems, where data allocation for each client is drawn from a Dirichlet distribution with parameter $\alpha = 0.1$. This is considered a rather challenging regime due to high-class imbalance. Every result shows the average across three simulation runs with different seeds. Details on the simulation setup and the network architectures are deferred to Appendix F. Consistently throughout all experiments, our proposed methods provide order-wise improvements in the communication cost while achieving state-of-the-art accuracies.

We plot in Fig. 1 the test accuracies for all the schemes as a function of the total communication cost in bits per parameter and per global iteration. While all the schemes achieve approximately the same maximum test accuracy, BiCompFL-GR and BiCompFL-PR require substantially less communication. Hence, when the bandwidths of uplink and downlink transmissions are limited, both variations of the proposed method achieve better test accuracies. Turning our focus to the different variations of our scheme, it can be observed that, without partitioning the model for downlink compression, BiCompFL-PR convergences significantly slower than BiCompFL-GR for any block allocation method. This highlights the intuition above that the additional MRC step in downlink incurs further noise, which reduces the convergence speed. However, when we partition the model in the downlink and only send disjoint parts to each client through MRC (BiCompFL-PR-Fixed-SplitDL), the downlink communication cost reduces by a factor of n . In the regime of Fashion MNIST with uniform data allocation, this comes without performance degradation, and is hence the method of choice in this regime. We additionally simulated BiCompFL-GR with the suboptimal implementation (BiCompFL-GR-Reconst-Fixed), in which the federator first reconstructs the global model, and then performs an additional MRC step for downlink transmission. This naturally reduces the convergence speed per iteration without gains in the communication cost. Hence, justifying the choice of BiCompFL-GR. We show that, in conventional FL, BiCompFL-GR-CFL substantially reduces the communication cost without loss in performance.

In some cases, especially for non-i.i.d. data, we even observe improved performance, which we attribute to implicit regularization. Note that BiCompFL-GR-CFL provides improvements even without error-feedback or momentum. However, our method is fully compatible with such techniques, and can be used as a plug-in approach to further minimize the communication cost in many existing schemes. We study the convergence in Section 5.

We plot in Fig. 2(a) the average bitrate of each scheme over the maximum test accuracy for MNIST and 4CNN. The average bitrate is reduced by more than a factor of 1000 compared to FedAvg, and more than a **factor of 32** compared to DOUBLESQUEEZE, NEOLITHIC and LIEC, which perform best among the conventional bi-directional compression methods.

We perform the same study for non-i.i.d. data allocation according to a Dirichlet distribution with parameter $\alpha = 0.1$, and show the maximum test accuracies over the average bitrate in Fig. 2(b). It can be found that partitioning the model in BiCompFL-PR worsens the final accuracy of the model. While the model converges faster, it does not achieve the same accuracies as BiCompFL-GR and BiCompFL-PR without partitioning. This hints towards hybrid schemes for BiCompFL-PR, where the training begins with partitioning on the downlink, and the scheme later switches to full transmission.

In Fig. 2(c), we provide the results for CIFAR-10 and uniform data allocation. BiCompFL-GR and BiCompFL-PR both achieve better results with a bitrate **smaller by a factor of 5** than the best baselines. More detailed numerical results can be found in Appendices I and J.

The adaptive block allocation (Adaptive) of Isik et al. (2024) saves communication costs in many settings and provides better performance than the fixed block allocation (Fixed), due to more accurate MRC tailored to the exact divergences. The proposed low complexity adaptive strategy based on the average KL-divergence (Adaptive-Avg) per block can additionally save in communication (and compu-

tation) with no or little performance degradation. We refer the reader to Appendix I for further extensive experiments, graphs for accuracies over epochs, separate studies of uplink and downlink costs, and comparisons for the case of an available broadcast channel from federator to the clients. Further, we refer to Appendix J for various ablation studies analyzing the sensitivity of BiCompFL with respect to the choices of the priors, n , n_{DL} , n_{IS} , and the block size d/B .

5 Theoretical Results

Convergence. In stochastic FL, the exact dynamics of the system over time are challenging to analyze due to the round-dependent interplay of the learning procedure with the transmission noise. However, when using BiCompFL for conventional FL with stochastic quantization (cf. BiCompFL-GR-CFL), convergence guarantees can be given. For a comprehensive understanding, we prove the convergence for a general and widely used class of stochastic quantizers $Q_s(\cdot)$, which are natively unbiased. $Q_s(\cdot)$ takes as input the entry g_e of a gradient vector $\mathbf{g} \in \mathbb{R}^d$ and operates as follows. Let s be the number of quantization intervals, and let $0 \leq \tau_e < s$ be an integer such that $\frac{\tau_e}{s} \leq \frac{|g_e|}{\|\mathbf{g}\|} \leq \frac{\tau_e+1}{s}$, then $Q_s(g_e)$ outputs $\|\mathbf{g}\| \cdot \text{sign}(g_e)(\tau_e + 1)/s$ with probability $\frac{|g_e|}{\|\mathbf{g}\|}s - \tau_e$, and $\|\mathbf{g}\| \cdot \text{sign}(g_e)\tau_e/s$ otherwise. $Q_s(\cdot)$ is unbiased, i.e., $\mathbb{E}[Q_s(\mathbf{x})] = \mathbf{x}$, and its variance satisfies $\mathbb{E}[\|Q_s(\mathbf{x}) - \mathbf{x}\|^2] \leq \min\{d/s^2, \sqrt{d}/s\} \|\mathbf{x}\|_2^2$ (Alistarh et al., 2017).

Replacing stochastic SignSGD by $Q_s(\cdot)$ in BiCompFL-GR-CFL, the posterior is given by a Bernoulli distribution with parameter $q_{i,e}^t = \frac{|g_{i,e}^t|}{\|g_i^t\|}s - \tau_e$. The values $\|\mathbf{g}\|$, $\text{sign}(\mathbf{g})$, and τ_e can be encoded independently, e.g., using Elias coding. With a slight abuse of notation, let $\mathcal{C}_{\text{mrc}}(Q_s(\cdot), \cdot)$ denote the composition of $Q_s(\cdot)$ and MRC with n_{IS} samples per entry. The compression $\mathcal{C}_{\text{mrc}}(Q_s(g_i^t), \cdot)$ takes a gradient g_i^t and outputs samples from a distribution close to $Q_s(g_i^t)$, and falls in the class of biased compressors. We can prove the following contraction property for $\mathcal{C}_{\text{mrc}}(Q_s(\cdot), \cdot)$, which will facilitate convergence analysis. A prominent biased contractive compressor is TopK.

Lemma 1. *For any $\mathbf{x} \in \mathbb{R}^d$ and corresponding posterior q following $Q_s(\mathbf{x})$, and a prior $p \in [0, 1]^d$, let $\bar{\Delta} := \max_{e \in [d]} \frac{q_e}{p_e} - \frac{1-q_e}{1-p_e}$, $\bar{\Delta}' := \max_{e \in [d]} q_e \left(\frac{p_e}{q_e} + \frac{1-p_e}{1-q_e} \right)$, and $\bar{p} := \max_{e \in [d]} p_e$. The compressor $\mathcal{C}_{\text{mrc}}(Q_s(\cdot))$ satisfies the following contraction property for $n_{\text{IS}} = \mathcal{O}(\max\{\sqrt{2\bar{\Delta}'}, \log(6\bar{p}(\bar{\Delta} + \bar{\Delta}'))\})\sqrt{6\bar{p}(\bar{\Delta} + \bar{\Delta}^2)}$ and $s \geq \sqrt{2d}$:*

$$\mathbb{E}[\|\mathcal{C}_{\text{mrc}}(Q_s(\mathbf{x})) - \mathbf{x}\|^2] \leq (1 - \delta)\|\mathbf{x}\|^2,$$

$$\text{for } \delta = 1 - \frac{d}{s^2} \left(1 + \frac{\bar{\Delta}'}{n_{\text{IS}}^2} + \mathcal{O} \left((\bar{\Delta} + \bar{\Delta}^2) \sqrt{\frac{6\bar{p} \log(2n_{\text{IS}})}{n_{\text{IS}}}} \right) \right).$$

The underlying core result is a refinement of the MRC analysis, cf. Lemma 2 (Appendix B). Hence, for sufficiently large n_{IS} , the compressor $\mathcal{C}_{\text{mrc}}(Q_s(\cdot), \cdot)$ can be used as an alternative to common compressors such as $Q_s(\cdot)$. The use of MRC introduces a bias into the otherwise unbiased stochastic quantization. Based on the contraction property in Lemma 1, standard convergence results follow easily, cf. Appendix C.

Communication Cost. We continue to analyze the communication cost in a specific iteration t and comment on the inter-round dependency later. When the latest global model estimate $\hat{\theta}_{i,t}$ is chosen as a prior in MRC, the cost of communication on the uplink is mainly determined by how far the model evolves during the client's training, i.e., $d_{\text{KL}}(q_i^t \| p_{i,u}^t) = d_{\text{KL}}(q_i^t \| \hat{\theta}_{i,t})$. After communicating samples of the posteriors, the federator obtains an estimate \hat{q}_i^t for all $i \in [n]$. The cost of communication on the downlink to client i is then determined by $d_{\text{KL}}(\frac{1}{n} \sum_{i=1}^n \hat{q}_i^t \| \hat{\theta}_{i,t})$. While $d_{\text{KL}}(q_i^t \| \hat{\theta}_{i,t})$ depends on the progress during client training, the core challenge is to bound the expected KL-divergence of each model estimate $d_{\text{KL}}(\hat{q}_i^t \| \hat{\theta}_{i,t})$ in the presence of potentially different priors, i.e., $\hat{\theta}_{i,t} \neq \hat{\theta}_{j,t}$, $i \neq j$. For each client i , the overall communication cost is in the order of

$$n_{\text{DL}} \exp \left(d_{\text{KL}} \left(\frac{1}{n} \sum_{i=1}^n \hat{q}_i^t \| p_{i,d}^t \right) \right) + n_{\text{UL}} \exp \left(d_{\text{KL}}(q_i^t \| p_{i,u}^t) \right).$$

We will next quantify $d_{\text{KL}}(\frac{1}{n} \sum_{i=1}^n \hat{q}_i^t \| \hat{\theta}_{i,t})$ for the case $p_{i,u}^t = p_{i,d}^t$, however, the analysis can be extended to $p_{i,u}^t \neq p_{i,d}^t$ by an additional assumption on the divergence between the two priors.

For the theoretical analysis, we focus on the scalar case for a single iteration t , where client $i \in [n]$ has a posterior Q_i , and the federator and client i share a common prior P_i , both are Bernoulli distributions with parameters q_i and p_i , respectively. In the context of FL, the client locally trains P_i and results with Q_i . According to Chatterjee & Diaconis (2018) and the multi-client extension of Isik et al. (2024), the communication cost in the uplink is determined by $\exp(d_{\text{KL}}(Q_i \| P_i))$. After uplink transmission, the federator obtains an estimate \hat{q}_i of q_i ; and hence, the updated global model is given by $\frac{1}{n} \sum_{i=1}^n \hat{q}_i$. The communication cost in the downlink for client i is determined by $d_{\text{KL}}(\frac{1}{n} \sum_{i=1}^n \hat{q}_i \| p_i)$. Our theoretical contribution is a new high probability upper bound on this quantity, which refines previous MRC analysis, for the special case of Bernoulli distributions. Let X be a Bernoulli sample obtained through MRC. As an initial step, we derive an upper bound on the difference between q_i and the probability $\Pr(X) = 1$ that the samples are drawn from, which vanishes when $p_i = q_i$ (and hence $d_{\text{KL}}(q_i \| p_i) = 0$). We note that the bound of Chatterjee & Diaconis (2018, Theorem 1.1) does not satisfy this natural property. We formally

state the result in Proposition 1 in Appendix B, which, however, does not yet capture the dependency on the number of samples n_{IS} used in MRC to sample an index. We refine Proposition 1 with Lemma 2 (cf. Appendix B), which additionally captures this dependency, and will allow us to derive an upper bound on $d_{KL}(\frac{1}{n} \sum_{i=1}^n \hat{q}_i || p_i)$. Lemma 2 is of independent interest and can be seen as a refinement of the analysis by Chatterjee & Diaconis (2018) for Bernoulli distributions. It is required to prove Theorem 1.

For the statement of the following theorem, we assume that the progress by one local client training is bounded by $|q_j - p_j| \leq \rho$ for all $j \in [n]$. Using Pinsker’s inequality to bound $|q_j - p_j| \leq \frac{1}{2} \sqrt{d_{KL}(q_j || p_j) / 2}$, this is a natural assumption given from the KL-proximity term of mirror descent (for one local iteration), and can be strictly enforced through the projection of q_j onto a KL ball around p_j of fixed divergence. We assume that the difference between the clients’ priors, i.e., their global model estimates in our algorithms, are bounded as $|p_i - p_j| \leq \zeta$ for all $i, j \in [n]$.

Theorem 1. *Assume $p_j > \zeta$ for all $j \in [n]$, for $\Delta_j := \frac{q_j}{p_j - \zeta} - \frac{1 - q_j}{1 - p_j + \zeta}$ and $\Delta'_j := q_j (\frac{p_j + \zeta}{q_j} + \frac{1 - p_j + \zeta}{1 - q_j})$, with probability $1 - \delta'$, the global model divergence $d_{KL}(\frac{1}{n} \sum_{j=1}^n \hat{q}_j || p_i)$ is upper bounded by*

$$\sum_{j=1}^n \frac{2}{n \min\{p_i, 1 - p_i\}} \left(\frac{\Delta'_j}{n_{IS}^2} + \sqrt{\frac{\ln(2/\delta')}{2n_{UL}}} + \rho + \zeta^2 + \right. \\ \left. + \mathcal{O}\left((\Delta_j + \Delta_j^2) \sqrt{\frac{6(p_i + \zeta) \log(2n_{IS})}{n_{IS}}} \right) \right)$$

By Chatterjee & Diaconis (2018), this provides an immediate bound on the cost of downlink transmission. The bound applies to both algorithms BiCompFL-PR and BiCompFL-GR. However, when all priors p_j are the same (such as in BiCompFL-GR-Reconst), i.e., $\zeta = 0$, the bound simplifies accordingly. The explicit dependency on the factor $1/\sqrt{n_{UL}}$ reflects the interplay between uplink and downlink cost. The parameter ζ gives rise to an inter-round dependency of the communication cost. The more accurate the estimation of the global model in the previous iteration (given the priors are chosen as $\hat{\theta}_{i,t}$), the smaller ζ , and hence the lower the transmission cost in the subsequent iteration. The proofs of Proposition 1, Lemma 2, and Theorem 1 can be found in Appendix B.

6 Related Work

Followed by the introduction of FL by McMahan et al. (2017), lossy compression of gradients or model updates has been a long studied narrative in FL, with prominent representatives such as SignSGD, also known as 1-bit Stochastic Gradient Descent (SGD) (Seide et al., 2014), QSGD (Alistarh et al., 2017), TernGrad (Wen et al., 2017),

SignSGD with error feedback (Karimireddy et al., 2019), vector-quantized SGD (Gandikota et al., 2021) and natural compression (Horvoth et al., 2022). Such methods retain satisfactory final model accuracy even with aggressive quantization. Sparsification-based methods have also been considered as alternatives, e.g., TopK (Wangni et al., 2018; Shi et al., 2019). The importance of bi-directional gradient compression in many settings was outlined by Philippenko & Dieuleveut (2020). Many schemes were proposed that leverage combinations of gradient compression in the uplink and downlink, error-feedback, and momentum, e.g., Mem-SGD (Stich et al., 2018), DoubleSqueeze (Tang et al., 2019), block-wise SignSGD with momentum (Zheng et al., 2019), communication-efficient SGD with error reset (Cser) (Xie et al., 2020), Artemis (Philippenko & Dieuleveut, 2020), Neolithic (Huang et al., 2022), DoCoFL (Dorfman et al., 2023), EF21-P and friends (Gruntkowska et al., 2023), 2Direction (Tyurin & Richtarik, 2023), M3 (Gruntkowska et al., 2024), and LIEC (Cheng et al., 2024). With the exception of the methods MCM (Philippenko & Dieuleveut, 2021) and M3 (Gruntkowska et al., 2024), each client receives the same broadcast, potentially compressed, global gradient or model update. Isik et al. (2024) studied uplink compression for stochastic FL and showed significant communication reduction with competitive performance. Their framework, termed KLMS, applies to a variety of stochastic compressors and to Bayesian FL settings, e.g., QLSD (Vono et al., 2022). The compression is based on importance sampling and MRC, thoroughly studied by Chatterjee & Diaconis (2018) and Havasi et al. (2019). Such methods, known as relative entropy coding, have been used in FL in conjunction with differential privacy, cf. DP-REC (Triastcyn et al., 2022).

Since the lottery ticket hypothesis (Frankle & Carbin, 2019), finding sparse subnetworks of neural networks that achieve satisfactory accuracy was investigated. Ramanujan et al. (2020) showed that randomly weighted networks contain suitable subnetworks of large neural networks capable of achieving competitive performance. Isik et al. (2023) formulated a probabilistic method of training neural network masks collaboratively in an FL context.

7 Conclusion

We illuminated the problem of bi-directional compression in stochastic FL using the specific instance of federated probabilistic mask training, which we showed to inherently optimize both the learning objective and the communication costs. By leveraging side-information through carefully chosen prior distributions, the total communication costs can be reduced by factors between 5 and 32 compared to non-stochastic FL baselines while achieving state-of-the-art accuracies on classification tasks in both homogeneous and heterogeneous FL regimes. We thereby close the

gap of downlink compression for stochastic FL and complement the existing literature on bi-directional compression for standard FL. Applying our methods to stochastic quantization in conventional FL, we paved the way to convergence analysis for MRC-based compression. Allowing different priors among all clients, this work opens the door to studying compression under side-information in *decentralized stochastic FL*, where a central coordinator is missing. Our theoretical results are of independent interest and may be applied in various scenarios where MRC is used.

Impact Statement

This paper presents work whose goal is to advance the field of Machine Learning. There are many potential societal consequences of our work, none which we feel must be specifically highlighted here.

References

- Afshin Abdi and Faramarz Fekri. Nested dithered quantization for communication reduction in distributed training. *arXiv preprint arXiv:1904.01197*, 2019.
- Dan Alistarh, Demjan Grubic, Jerry Li, Ryota Tomioka, and Milan Vojnovic. QSGD: Communication-efficient SGD via gradient quantization and encoding. In *Advances in Neural Information Processing Systems*, volume 30, 2017.
- Mohammad Mohammadi Amiri, Deniz Gunduz, Sanjeev R. Kulkarni, and H. Vincent Poor. Federated learning with quantized global model updates. *arXiv preprint arXiv:2006.10672*, 2020.
- Sourav Chatterjee and Persi Diaconis. The sample size required in importance sampling. *The Annals of Applied Probability*, 28(2):1099–1135, 2018.
- Yifei Cheng, Li Shen, Linli Xu, Xun Qian, Shiwei Wu, Yiming Zhou, Tie Zhang, Dacheng Tao, and Enhong Chen. Communication-efficient distributed learning with local immediate error compensation. *arXiv preprint arXiv:2402.11857*, 2024.
- Thomas Cover and Joy A Thomas. *Elements of information theory*. Wiley-Interscience, 2006.
- Ron Dorfman, Shay Vargaftik, Yaniv Ben-Itzhak, and Kfir Yehuda Levy. DoCoFL: Downlink compression for cross-device federated learning. In *International Conference on Machine Learning*, pp. 8356–8388, 2023.
- Jonathan Frankle and Michael Carbin. The lottery ticket hypothesis: Finding sparse, trainable neural networks. In *International Conference on Learning Representations*, 2019.
- Venkata Gandikota, Daniel Kane, Raj Kumar Maity, and Arya Mazumdar. vqSGD: Vector quantized stochastic gradient descent. In *International Conference on Artificial Intelligence and Statistics*, volume 130, pp. 2197–2205, 2021.
- Kaja Gruntkowska, Alexander Tyurin, and Peter Richtárik. EF21-P and friends: Improved theoretical communication complexity for distributed optimization with bidirectional compression. In *International Conference on Machine Learning*, pp. 11761–11807, 2023.
- Kaja Gruntkowska, Alexander Tyurin, and Peter Richtárik. Improving the worst-case bidirectional communication complexity for nonconvex distributed optimization under function similarity. *arXiv preprint arXiv:2402.06412*, 2024.
- Marton Havasi, Robert Peharz, and José Miguel Hernández-Lobato. Minimal random code learning: Getting bits back from compressed model parameters. In *International Conference on Learning Representations*, 2019.
- Samuel Horváth, Chen-Yu Ho, Ludovit Horvath, Atal Narayan Sahu, Marco Canini, and Peter Richtarik. Natural compression for distributed deep learning. In *Proceedings of Mathematical and Scientific Machine Learning*, volume 190, pp. 129–141, 2022.
- Xinmeng Huang, Yiming Chen, Wotao Yin, and Kun Yuan. Lower bounds and nearly optimal algorithms in distributed learning with communication compression. *Advances in Neural Information Processing Systems*, 35: 18955–18969, 2022.
- Berivan Isik, Francesco Pase, Deniz Gunduz, Tsachy Weissman, and Zorzi Michele. Sparse random networks for communication-efficient federated learning. In *International Conference on Learning Representations*, 2023.
- Berivan Isik, Francesco Pase, Deniz Gunduz, Sanmi Koyejo, Tsachy Weissman, and Michele Zorzi. Adaptive compression in federated learning via side information. In *International Conference on Artificial Intelligence and Statistics*, pp. 487–495, 2024.
- Sai Praneeth Karimireddy, Quentin Rebjock, Sebastian Stich, and Martin Jaggi. Error feedback fixes SignSGD and other gradient compression schemes. In *International Conference on Machine Learning*, volume 97, pp. 3252–3261, 2019.
- Diederik P Kingma and Jimmy Ba. Adam: A method for stochastic optimization. In *International Conference on Learning Representations*, 2015.

- Y. Lecun, L. Bottou, Y. Bengio, and P. Haffner. Gradient-based learning applied to document recognition. *Proceedings of the IEEE*, 86(11):2278–2324, 1998.
- Brendan McMahan, Eider Moore, Daniel Ramage, Seth Hampson, and Blaise Aguera y Arcas. Communication-Efficient Learning of Deep Networks from Decentralized Data. In *International Conference on Artificial Intelligence and Statistics*, volume 54, pp. 1273–1282, 2017.
- Constantin Philippenko and Aymeric Dieuleveut. Bidirectional compression in heterogeneous settings for distributed or federated learning with partial participation: tight convergence guarantees. *arXiv preprint arXiv:2006.14591*, 2020.
- Constantin Philippenko and Aymeric Dieuleveut. Preserved central model for faster bidirectional compression in distributed settings. *Advances in Neural Information Processing Systems*, 34:2387–2399, 2021.
- Vivek Ramanujan, Mitchell Wortsman, Aniruddha Kembhavi, Ali Farhadi, and Mohammad Rastegari. What’s hidden in a randomly weighted neural network? In *IEEE/CVF conference on computer vision and pattern recognition*, pp. 11893–11902, 2020.
- Peter Richtárik, Igor Sokolov, and Ilyas Fatkhullin. Ef21: A new, simpler, theoretically better, and practically faster error feedback. *Advances in Neural Information Processing Systems*, 34:4384–4396, 2021.
- Frank Seide, Hao Fu, Jasha Droppo, Gang Li, and Dong Yu. 1-bit stochastic gradient descent and its application to data-parallel distributed training of speech DNNs. In *Interspeech*, pp. 1058–1062, 2014.
- Shaohuai Shi, Qiang Wang, Kaiyong Zhao, Zhenheng Tang, Yuxin Wang, Xiang Huang, and Xiaowen Chu. A distributed synchronous SGD algorithm with global top-k sparsification for low bandwidth networks. In *International Conference on Distributed Computing Systems (ICDCS)*, pp. 2238–2247, 2019.
- Rajan Srinivasan. *Importance sampling: Applications in communications and detection*. Springer Science & Business Media, 2002.
- Sebastian U Stich, Jean-Baptiste Cordonnier, and Martin Jaggi. Sparsified SGD with memory. *Advances in Neural Information Processing Systems*, 31, 2018.
- Hanlin Tang, Chen Yu, Xiangru Lian, Tong Zhang, and Ji Liu. Doublesqueeze: Parallel stochastic gradient descent with double-pass error-compensated compression. In *International Conference on Machine Learning*, pp. 6155–6165, 2019.
- Aleksei Triastcyn, Matthias Reisser, and Christos Louizos. DP-REC: Private & communication-efficient federated learning, 2022.
- Alexander Tyurin and Peter Richtárik. 2Direction: theoretically faster distributed training with bidirectional communication compression. In *Conference on Neural Information Processing Systems*, 2023.
- Maxime Vono, Vincent Plassier, Alain Durmus, Aymeric Dieuleveut, and Eric Moulines. QLSGD: quantised langevin stochastic dynamics for bayesian federated learning. In *International Conference on Artificial Intelligence and Statistics*, pp. 6459–6500, 2022.
- Jianqiao Wangni, Jialei Wang, Ji Liu, and Tong Zhang. Gradient sparsification for communication-efficient distributed optimization. *Advances in Neural Information Processing Systems*, 31, 2018.
- Nir Weinberger and Michal Yemini. Multi-armed bandits with self-information rewards. *IEEE Transactions on Information Theory*, 2023.
- Jie Wen, Zhixia Zhang, Yang Lan, Zhihua Cui, Jianghui Cai, and Wensheng Zhang. A survey on federated learning: challenges and applications. *International Journal of Machine Learning and Cybernetics*, 14(2):513–535, 2023.
- Wei Wen, Cong Xu, Feng Yan, Chunpeng Wu, Yandan Wang, Yiran Chen, and Hai Li. TernGrad: Ternary gradients to reduce communication in distributed deep learning. In *Advances in Neural Information Processing Systems*, volume 30, 2017.
- Cong Xie, Shuai Zheng, Sanmi Koyejo, Indranil Gupta, Mu Li, and Haibin Lin. Cser: Communication-efficient sgd with error reset. *Advances in Neural Information Processing Systems*, 33:12593–12603, 2020.
- Chen Zhang, Yu Xie, Hang Bai, Bin Yu, Weihong Li, and Yuan Gao. A survey on federated learning. *Knowledge-Based Systems*, 216:106775, 2021.
- Shuai Zheng, Ziyue Huang, and James Kwok. Communication-efficient distributed blockwise momentum SGD with error-feedback. *Advances in Neural Information Processing Systems*, 32, 2019.

A Reproducibility

In addition to the algorithmic details and the clients' training procedure function (cf. Algorithms 1, 2 and 3), we provide in Section 4 the most important hyperparameters used in our experiments, such as local and global iterations, and data allocation. Further parameter information, such as batch size, learning rates and the choice of the optimizer can be found in Appendix I, together with details on the neural network architectures and the hardware cluster used for running the experiments. Particularities of the block allocation required for the operation of our schemes are described in Appendix E. All assumptions required for the theoretical analysis are stated in Section 5. Full proofs of all claims, including formal statements, can be found in Appendix B.

B Proofs and Intermediate Results

In the following, we provide the formal statements of Proposition 1 and Lemma 2 including their proofs. Parts of the proof of Proposition 1 will be used to prove Lemma 2. We prove Theorem 1 afterward.

Proposition 1. *For a sample X_ℓ transmitted by MRC with posterior and prior Bernoulli distributions with parameters q and p , we have*

$$|\Pr(X_\ell = 1) - q| \leq q \left(\max \left\{ \frac{p}{q}, \frac{1-p}{1-q}, \frac{q}{p}, \frac{1-q}{1-p} \right\} - 1 \right).$$

Proof of Proposition 1. Assume a party wants to sample from a Bernoulli distribution Q with parameter q , which is held by another party. Both parties share a common prior P in the form of a Bernoulli distribution with parameter p and have access to shared randomness. Fix any sample index ℓ for the moment (this index will be needed for the proof of Theorem 1). Both parties sample $K n_{\text{IS}}$ i.i.d. samples $X_{\ell,i} \sim P$ for $i \in [n_{\text{IS}}]$ independently and identically from P . The party holding Q constructs an auxiliary distribution

$$W_\ell(i) = \frac{Q(X_{\ell,i})/P(X_{\ell,i})}{\sum_{i=1}^{n_{\text{IS}}} Q(X_{\ell,i})/P(X_{\ell,i})},$$

from which it samples to obtain an index I_ℓ . The index is transmitted to the other party, which reconstructs the corresponding sample X_{ℓ,I_ℓ} .

To bound the difference $|\Pr(X_\ell = 1) - q|$, i.e., the target Bernoulli parameter compared to the parameter which the sample is drawn from, by the independence of the samples X_{ℓ,I_ℓ} for different ℓ , we focus on a single sample $\ell \in [K]$, for which it holds that

$$\begin{aligned} & \Pr(X_{\ell,I_\ell} = 1) \\ &= \sum_{i=1}^{n_{\text{IS}}} \sum_{\{x_1, \dots, x_{n_{\text{IS}}}: x_i = i\}} \Pr(X_{\ell,1} = x_1, \dots, X_{\ell,n_{\text{IS}}} = x_{n_{\text{IS}}}) \Pr(I_\ell = i \mid X_{\ell,1} = x_1, \dots, X_{\ell,n_{\text{IS}}} = x_{n_{\text{IS}}}) \\ &\stackrel{(a)}{=} n_{\text{IS}} \sum_{\{x_2, \dots, x_{n_{\text{IS}}}\}} \Pr(X_{\ell,1} = 1, X_{\ell,2} = x_2, \dots, X_{\ell,n_{\text{IS}}} = x_{n_{\text{IS}}}) \\ &\quad \cdot \Pr(I_\ell = 1 \mid X_{\ell,1} = 1, X_{\ell,2} = x_2, \dots, X_{\ell,n_{\text{IS}}} = x_{n_{\text{IS}}}) \\ &\stackrel{(b)}{=} n_{\text{IS}} \sum_{L=0}^{n_{\text{IS}}-1} \sum_{\{x_2, \dots, x_{n_{\text{IS}}}: \sum_{i=2}^{n_{\text{IS}}} x_i = L\}} \Pr(X_{\ell,1} = 1, X_{\ell,2} = x_2, \dots, X_{\ell,n_{\text{IS}}} = x_{n_{\text{IS}}}) \\ &\quad \cdot \Pr(I_\ell = 1 \mid X_{\ell,1} = 1, X_{\ell,2} = x_2, \dots, X_{\ell,n_{\text{IS}}} = x_{n_{\text{IS}}}), \end{aligned}$$

where (a) follows from symmetry, (b) follows since by permutation invariance, the inner probability only depends on the number of ones in $\{x_2, \dots, x_{n_{\text{IS}}}\}$.

The inner probability is given by the distribution $W_\ell(i)$. Given that $X_{\ell,1} = 1$ and that $\sum_{i=2}^{n_{\text{IS}}} X_{\ell,i} = L$, it holds that

$$\sum_{i=1}^{n_{\text{IS}}} Q(X_{\ell,i})/P(X_{\ell,i}) = (L+1) \cdot \frac{q}{p} + (n_{\text{IS}} - L - 1) \cdot \frac{1-q}{1-p}.$$

Hence,

$$\Pr(I_\ell = 1 \mid X_{\ell,1} = 1, X_{\ell,2} = x_2, \dots, X_{\ell,n_{\text{IS}}} = x_{n_{\text{IS}}}) = \frac{\frac{q}{p}}{(\text{L} + 1) \cdot \frac{q}{p} + (n_{\text{IS}} - \text{L} - 1) \cdot \frac{1-q}{1-p}},$$

which is independent of the exact choice of $\{x_2, \dots, x_{n_{\text{IS}}}\}$ given their sum $\sum_{i=2}^{n_{\text{IS}}} X_{\ell,i} = \text{L}$. Since $\Pr(X_{\ell,1} = 1, X_{\ell,2} = x_2, \dots, X_{\ell,n_{\text{IS}}} = x_{n_{\text{IS}}}) = p^{\text{L}+1}(1-p)^{n_{\text{IS}}-\text{L}-1}$ by the Bernoulli distribution assumption, we have

$$\Pr(X_{\ell,I_\ell} = 1) = n_{\text{IS}} \sum_{\text{L}=0}^{n_{\text{IS}}-1} \binom{n_{\text{IS}}-1}{\text{L}} p^{\text{L}+1} (1-p)^{n_{\text{IS}}-\text{L}-1} \frac{\frac{q}{p}}{(\text{L} + 1) \cdot \frac{q}{p} + (n_{\text{IS}} - \text{L} - 1) \cdot \frac{1-q}{1-p}},$$

Defining a binary random variable M with sample space $\left\{\frac{q}{p}, \frac{1-q}{1-p}\right\}$, for a Bernoulli distribution $\text{Ber}\left(\frac{\text{L}+1}{n_{\text{IS}}}\right)$ with success probability parameter $\frac{\text{L}+1}{n_{\text{IS}}}$, where a success refers to the outcome $M = \frac{q}{p}$, we can write that

$$\begin{aligned} \Pr(X_{\ell,I_\ell} = 1) &= q \cdot \sum_{\text{L}=0}^{n_{\text{IS}}-1} \binom{n_{\text{IS}}-1}{\text{L}} p^{\text{L}+1} (1-p)^{n_{\text{IS}}-\text{L}-1} \frac{1}{\frac{\text{L}+1}{n_{\text{IS}}} \frac{q}{p} + \frac{n_{\text{IS}}-\text{L}-1}{n_{\text{IS}}} \frac{1-q}{1-p}} \\ &= q \cdot \mathbb{E} \left[\frac{1}{\frac{\text{L}+1}{n_{\text{IS}}} \frac{q}{p} + \frac{n_{\text{IS}}-\text{L}-1}{n_{\text{IS}}} \frac{1-q}{1-p}} \right] = q \mathbb{E} \left[\frac{1}{\mathbb{E}_{\text{Ber}\left(\frac{\text{L}+1}{n_{\text{IS}}}\right)}[M]} \right] \\ &\stackrel{(a)}{\leq} q \mathbb{E} \left[\mathbb{E}_{\text{Ber}\left(\frac{\text{L}+1}{n_{\text{IS}}}\right)} \left[\frac{1}{M} \right] \right], \end{aligned} \quad (1)$$

where the outer expectation is over the binomial distribution with $n_{\text{IS}} - 1$ trials and success probability p , i.e., $\text{L} \sim \text{Binomial}(n_{\text{IS}} - 1, p)$, and where (a) follows from Jensen's inequality over the inner expectation. Hence,

$$\begin{aligned} \Pr(X_{\ell,I_\ell} = 1) - q &= q \left(\frac{\Pr(X_{\ell,I_\ell} = 1)}{q} - 1 \right) \\ &\leq q \left(\mathbb{E} \left[\mathbb{E}_{\text{Ber}\left(\frac{\text{L}+1}{n_{\text{IS}}}\right)} \left[\frac{1}{M} \right] \right] - 1 \right) \end{aligned} \quad (2)$$

Since $\frac{1}{\mathbb{E}_{\text{Ber}\left(\frac{\text{L}+1}{n_{\text{IS}}}\right)}[M]} \geq 2 - \mathbb{E}_{\text{Ber}\left(\frac{\text{L}+1}{n_{\text{IS}}}\right)}[M]$, it also follows from (1) that

$$\begin{aligned} \Pr(X_{\ell,I_\ell} = 1) &= q \cdot \mathbb{E} \left[\frac{1}{\frac{\text{L}+1}{n_{\text{IS}}} \frac{q}{p} + \frac{n_{\text{IS}}-\text{L}-1}{n_{\text{IS}}} \frac{1-q}{1-p}} \right] = q \mathbb{E} \left[\frac{1}{\mathbb{E}_{\text{Ber}\left(\frac{\text{L}+1}{n_{\text{IS}}}\right)}[M]} \right] \\ &\geq q \mathbb{E} \left[2 - \mathbb{E}_{\text{Ber}\left(\frac{\text{L}+1}{n_{\text{IS}}}\right)}[M] \right], \end{aligned}$$

from which we have

$$\Pr(X_{\ell,I_\ell} = 1) - q \geq q \left(1 - \mathbb{E} \left[\mathbb{E}_{\text{Ber}\left(\frac{\text{L}+1}{n_{\text{IS}}}\right)}[M] \right] \right). \quad (3)$$

Combining the upper and lower bound in (2) and (3), respectively, we derive

$$\begin{aligned}
 |\Pr(X_{\ell, I_\ell} = 1) - q| &\leq q \left(\max \left\{ \mathbb{E} \left[1 - \mathbb{E}_{\text{Ber}(\frac{L+1}{n_{IS}})} [M] \right], \mathbb{E} \left[\mathbb{E}_{\text{Ber}(\frac{L+1}{n_{IS}})} \left[\frac{1}{M} \right] \right] \right\} - 1 \right) \\
 &\leq q \left(\mathbb{E} \left[\max \left\{ \mathbb{E}_{\text{Ber}(\frac{L+1}{n_{IS}})} [M], \mathbb{E}_{\text{Ber}(\frac{L+1}{n_{IS}})} \left[\frac{1}{M} \right] \right\} \right] - 1 \right) \\
 &\leq q \left(\mathbb{E} \left[\mathbb{E}_{\text{Ber}(\frac{L+1}{n_{IS}})} \left[\max \left\{ M, \frac{1}{M} \right\} \right] \right] - 1 \right) \\
 &\leq q \left(\mathbb{E} \left[\max \left\{ \frac{p}{q}, \frac{1-p}{1-q}, \frac{q}{p}, \frac{1-q}{1-p} \right\} \right] - 1 \right) \\
 &= q \left(\max \left\{ \frac{p}{q}, \frac{1-p}{1-q}, \frac{q}{p}, \frac{1-q}{1-p} \right\} - 1 \right).
 \end{aligned}$$

This concludes the proof. \square

Lemma 2. For a sample X_ℓ transmitted via MRC with posterior and prior being Bernoulli distributions with parameters q and p , $\Delta := \frac{q}{p} - \frac{1-q}{1-p}$ and $\Delta' := q \left(\frac{p}{q} + \frac{1-p}{1-q} \right)$, we have

$$|\Pr(X_\ell = 1) - q| \leq \frac{\Delta'}{n_{IS}^2} + \mathcal{O} \left((\Delta + \Delta^2) \sqrt{\frac{6p \log(2n_{IS})}{n_{IS}}} \right).$$

Proof of Lemma 2. The proof starts with the same derivations as for the proof of Proposition 1, which we follow until (1) to get

$$\Pr(X_{\ell, I_\ell} = 1) = q \mathbb{E} \left[\frac{1}{\mathbb{E}_{\text{Ber}(\frac{L+1}{n_{IS}})} [M]} \right]$$

Since L is a random quantity that follows a Binomial distribution, we bound $|\Pr(X_{\ell, I_\ell} = 1) - q|$ using a concentration bound on L . The relative (multiplicative) Chernoff bound states that

$$\begin{aligned}
 \Pr(|L - \varepsilon(n_{IS}p)| \geq \varepsilon n_{IS}p) &= \Pr(L - \varepsilon(n_{IS}p) \geq \varepsilon n_{IS}p) + \Pr(L - \varepsilon(n_{IS}p) \leq -\varepsilon n_{IS}p) \\
 &\leq 2 \exp \left(-\frac{\varepsilon^2 n_{IS}p}{3} \right)
 \end{aligned}$$

for any $\varepsilon \in [0, 1]$. Setting $\varepsilon = \sqrt{\frac{3 \log(2/\delta)}{n_{IS}p}}$ implies that

$$|L - n_{IS}p| \geq \sqrt{3n_{IS}p \log(2/\delta)}$$

with probability at most δ . Setting $\delta = \frac{1}{n_{IS}^2}$, we obtain for a concentration parameter² $\eta_\delta := \sqrt{\frac{6p \log(2n_{IS})}{n_{IS}}}$ that

$$\mathcal{E} := \{|L - n_{IS}p| \geq n_{IS}\eta_\delta\}$$

with probability $\Pr(\mathcal{E}) \leq \frac{1}{n_{IS}^2}$.

Then, we can write

$$\begin{aligned}
 \Pr(X_{\ell, I_\ell} = 1) &= q \mathbb{E} \left[\frac{1}{\mathbb{E}_{\text{Ber}(\frac{L+1}{n_{IS}})} [M]} \right] \\
 &= q \mathbb{E} \left[\frac{1}{\mathbb{E}_{\text{Ber}(\frac{L+1}{n_{IS}})} [M]} \cdot \mathbb{1}\{\mathcal{E}^c\} \right] + q \mathbb{E} \left[\frac{1}{\mathbb{E}_{\text{Ber}(\frac{L+1}{n_{IS}})} [M]} \cdot \mathbb{1}\{\mathcal{E}\} \right]
 \end{aligned} \tag{4}$$

²Note that we can assume $p + \eta_\delta \leq 1$ and $p - \eta_\delta \geq 0$, otherwise the concentration can be trivially bounded.

Assume for now that $q < p$ (we will later proof the opposite event), then $\frac{1}{\mathbb{E}_{\text{Ber}\left(\frac{L+1}{n_{\text{IS}}}\right)}[M]}$ is strictly non-increasing in L since $\frac{q}{p} < \frac{1-q}{1-p}$, and hence, when \mathcal{E}^c holds and hence L concentration around the average that

$$\begin{aligned} \frac{1}{\mathbb{E}_{\text{Ber}\left(\frac{L+1}{n_{\text{IS}}}\right)}[M]} &\leq \frac{1}{\mathbb{E}_{\text{Ber}\left(\frac{(L+1)\cdot(p-\eta_\delta)}{n_{\text{IS}}}\right)}[M]} \\ &= \frac{1}{\frac{(n_{\text{IS}}-1)(p-\eta_\delta)+1}{n_{\text{IS}}}\frac{q}{p} + \frac{n_{\text{IS}}-1-(n_{\text{IS}}-1)(p-\eta_\delta)}{n_{\text{IS}}}\frac{1-q}{1-p}} \\ &= \frac{1}{\left(p - \frac{p}{n_{\text{IS}}} + \frac{\eta_\delta}{n_{\text{IS}}} - \eta_\delta + \frac{1}{n_{\text{IS}}}\right)\frac{q}{p} + \left(1 - p - \frac{1}{n_{\text{IS}}} + \frac{p}{n_{\text{IS}}} + \eta_\delta - \frac{\eta_\delta}{n_{\text{IS}}}\right)\frac{1-q}{1-p}} \\ &= \frac{1}{1 + \left(\frac{q}{p} - \frac{1-q}{1-p}\right)\left(\frac{1-p+\eta_\delta-n\eta_\delta}{n_{\text{IS}}}\right)} \\ &= 1 + \sum_{\kappa=1}^{\infty} (-1)^\kappa \left(\frac{q}{p} - \frac{1-q}{1-p}\right)^\kappa \left(\frac{1-p+\eta_\delta-n\eta_\delta}{n_{\text{IS}}}\right)^\kappa, \end{aligned}$$

where the last step is by Taylor expansion. Using (4) and the monotonicity of $\frac{1}{\mathbb{E}_{\text{Ber}\left(\frac{L+1}{n_{\text{IS}}}\right)}[M]}$, we write

$$\begin{aligned} \Pr(X_{\ell, I_\ell} = 1) &= q \mathbb{E} \left[\frac{1}{\mathbb{E}_{\text{Ber}\left(\frac{L+1}{n_{\text{IS}}}\right)}[M]} \right] \\ &\leq q \left(1 + \sum_{\kappa=1}^{\infty} (-1)^\kappa \left(\frac{q}{p} - \frac{1-q}{1-p}\right)^\kappa \left(\frac{1-p+\eta_\delta-n\eta_\delta}{n_{\text{IS}}}\right)^\kappa \right) + q\delta\frac{p}{q}, \end{aligned}$$

and hence

$$\Pr(X_{\ell, I_\ell} = 1) - q \leq \delta p + (1-\delta) \sum_{\kappa=1}^{\infty} (-1)^\kappa \left(\frac{q}{p} - \frac{1-q}{1-p}\right)^\kappa \left(\frac{1-p+\eta_\delta-n\eta_\delta}{n_{\text{IS}}}\right)^\kappa$$

Similarly, we get by bounding $\frac{1}{\mathbb{E}_{\text{Ber}\left(\frac{L+1}{n_{\text{IS}}}\right)}[M]} \geq \frac{1}{\mathbb{E}_{\text{Ber}\left(\frac{(L+1)\cdot(p+\eta_\delta)}{n_{\text{IS}}}\right)}[M]}$ and using (4) that

$$\begin{aligned} \Pr(X_{\ell, I_\ell} = 1) - q &\geq \delta q \frac{1-p}{1-q} + (1-\delta) \sum_{\kappa=1}^{\infty} (-1)^\kappa \left(\frac{q}{p} - \frac{1-q}{1-p}\right)^\kappa \left(\frac{1-p-\eta_\delta+n\eta_\delta}{n_{\text{IS}}}\right)^\kappa \Leftrightarrow \\ q - \Pr(X_{\ell, I_\ell} = 1) &\leq -\delta q \frac{1-p}{1-q} + (1-\delta) \sum_{\kappa=1}^{\infty} (-1)^{\kappa+1} \left(\frac{q}{p} - \frac{1-q}{1-p}\right)^\kappa \left(\frac{1-p-\eta_\delta+n\eta_\delta}{n_{\text{IS}}}\right)^\kappa. \end{aligned}$$

When $p \leq q$, then $\frac{1}{\mathbb{E}_{\text{Ber}\left(\frac{L+1}{n_{\text{IS}}}\right)}[M]}$ is strictly non-decreasing, hence, under \mathcal{E} , we have

$$\frac{1}{\mathbb{E}_{\text{Ber}\left(\frac{L+1}{n_{\text{IS}}}\right)}[M]} \leq \frac{1}{\mathbb{E}_{\text{Ber}\left(\frac{(L+1)\cdot(p+\eta_\delta)}{n_{\text{IS}}}\right)}[M]} = 1 + \sum_{\kappa=1}^{\infty} (-1)^\kappa \left(\frac{q}{p} - \frac{1-q}{1-p}\right)^\kappa \left(\frac{1-p-\eta_\delta+n\eta_\delta}{n_{\text{IS}}}\right)^\kappa,$$

and thus from (4) that

$$\Pr(X_{\ell, I_\ell} = 1) - q \leq q\delta\frac{1-p}{1-q} + (1-\delta) \sum_{\kappa=1}^{\infty} (-1)^\kappa \left(\frac{q}{p} - \frac{1-q}{1-p}\right)^\kappa \left(\frac{1-p-\eta_\delta+n\eta_\delta}{n_{\text{IS}}}\right)^\kappa.$$

Similarly, we bound $\frac{1}{\mathbb{E}_{\text{Ber}\left(\frac{L+1}{n_{\text{IS}}}\right)}[\mathbb{M}]} \leq \frac{1}{\mathbb{E}_{\text{Ber}\left(\frac{(L+1) \cdot (p+\eta_\delta)}{n_{\text{IS}}}\right)}[\mathbb{M}]}$ to obtain

$$\begin{aligned} \Pr(X_{\ell, I_\ell} = 1) - q &\geq q\delta \frac{p}{q} + (1-\delta) \sum_{\kappa=1}^{\infty} (-1)^\kappa \left(\frac{q}{p} - \frac{1-q}{1-p}\right)^\kappa \left(\frac{1-p+\eta_\delta - n\eta_\delta}{n_{\text{IS}}}\right)^\kappa \Leftrightarrow \\ q - \Pr(X_{\ell, I_\ell} = 1) &\leq -q\delta \frac{p}{q} + (1-\delta) \sum_{\kappa=1}^{\infty} (-1)^{\kappa+1} \left(\frac{q}{p} - \frac{1-q}{1-p}\right)^\kappa \left(\frac{1-p+\eta_\delta - n\eta_\delta}{n_{\text{IS}}}\right)^\kappa \end{aligned}$$

Since $0 \leq p + \eta_\delta \leq 1$ and $1 \geq p - \eta_\delta \geq 0$ by an appropriate choice of the concentration intervals, we have by approximations up to second order terms that

$$\begin{aligned} |\Pr(X_{\ell, I_\ell} = 1) - q| &\leq q\delta \max\left\{\frac{p}{q}, \frac{1-p}{1-q}\right\} + \eta_\delta \left(\frac{q}{p} - \frac{1-q}{1-p}\right) + \left(\frac{q}{p} - \frac{1-q}{1-p}\right)^2 \mathcal{O}\left(\frac{1}{n_{\text{IS}}^2} + \eta_\delta^2\right) \\ &= \frac{q}{n_{\text{IS}}^2} \left(\frac{p}{q} + \frac{1-p}{1-q}\right) + \mathcal{O}\left(\left[\left(\frac{q}{p} - \frac{1-q}{1-p}\right) + \left(\frac{q}{p} - \frac{1-q}{1-p}\right)^2\right] \sqrt{\frac{6p \log(2n_{\text{IS}})}{n_{\text{IS}}}}\right). \end{aligned}$$

This concludes the proof. □

Proof of Lemma 1. Using Lemma 2, we can show the following. Recall the following probability law of the stochastic quantizer $Q_s(\cdot)$ (Alistarh et al., 2017) using $s > 0$ quantization intervals, which takes as input the entry x_e of a gradient $\mathbf{x} \in \mathbb{R}^d$ vector. Let $0 \leq \tau_e < s$ be an integer such that $\frac{\tau_e}{s} \leq \frac{|x_e|}{\|\mathbf{x}\|} \leq \frac{\tau_e+1}{s}$, then $Q_s(x_e)$ is defined as $\text{Ber}\left(\frac{|x_e|}{\|\mathbf{x}\|}s - \tau_e\right)$, which outputs $\|\mathbf{x}\| \cdot \text{sign}(x_e)(\tau_e + 1)/s$ in case of success, and $\|\mathbf{x}\| \cdot \text{sign}(x_e)\tau_e/s$ otherwise.

Focusing on an entry x_e , we prove a contraction property for MRC with stochastic quantization with posterior $q_e = \frac{|x_e|}{\|\mathbf{x}\|}s - \tau_e$, and an arbitrary prior p_e . In fact, the MRC methodology $\mathcal{C}_{\text{mrc}}(\cdot)$ leads to sampling from an approximate distribution with parameter \tilde{q}_e . To be more specific, $\mathcal{C}_{\text{mrc}}(x_e)$ outputs $\|\mathbf{x}\| \cdot \text{sign}(x_e)(\tau_e + 1)/s$ with probability \tilde{q}_e , and $\|\mathbf{x}\| \cdot \text{sign}(x_e)\tau_e/s$ with probability $1 - \tilde{q}_e$. We established in Lemma 2 an upper bound on $|q_e - \tilde{q}_e|$, which will be useful in the following.

To prove a contraction property of the kind

$$\mathbb{E}[\|\mathcal{C}_{\text{mrc}}(\mathbf{x}) - \mathbf{x}\|_2^2] \leq (1-\delta)\|\mathbf{x}\|^2,$$

we can write

$$\begin{aligned}
 \mathbb{E}[\|\mathcal{C}_{\text{mrc}}(\mathbf{x}) - \mathbf{x}\|^2] &= \mathbb{E}\left[\sum_{e=1}^d (\mathcal{C}_{\text{mrc}}(x_e) - x_e)^2\right] \\
 &= \|\mathbf{x}\|^2 \sum_{e=1}^d \mathbb{E}\left[\left(\frac{\mathcal{C}_{\text{mrc}}(x_e)}{\|\mathbf{x}\|} - \frac{x_e}{\|\mathbf{x}\|}\right)^2\right] \\
 &= \|\mathbf{x}\|^2 \sum_{e=1}^d \left[\tilde{q}_e \left(\frac{\text{sign}(x_e)(\tau_e + 1)}{s} - \frac{x_e}{\|\mathbf{x}\|}\right)^2 + (1 - \tilde{q}_e) \left(\frac{\text{sign}(x_e)\tau_e}{s} - \frac{x_e}{\|\mathbf{x}\|}\right)^2\right] \\
 &= \|\mathbf{x}\|^2 \sum_{e=1}^d \left[(\tilde{q}_e - q_e + q_e) \left(\frac{\tau_e + 1}{s} - \frac{|x_e|}{\|\mathbf{x}\|}\right)^2 + (1 - \tilde{q}_e - q_e + q_e) \left(\frac{\tau_e}{s} - \frac{|x_e|}{\|\mathbf{x}\|}\right)^2\right] \\
 &= \|\mathbf{x}\|^2 \sum_{e=1}^d \left[(q_e + \tilde{q}_e - q_e) \left(\left(\frac{\tau_e}{s} - \frac{|x_e|}{\|\mathbf{x}\|}\right)^2 + \frac{1}{s^2} + \frac{1}{s} \left(\frac{\tau_e}{s} - \frac{|x_e|}{\|\mathbf{x}\|}\right)\right) \right. \\
 &\quad \left. + (1 - q_e + q_e - \tilde{q}_e) \left(\frac{\tau_e}{s} - \frac{|x_e|}{\|\mathbf{x}\|}\right)^2\right] \\
 &= \|\mathbf{x}\|^2 \sum_{e=1}^d \left[(\tilde{q}_e - q_e) \left(\frac{1}{s^2} + \frac{1}{s} \left(\frac{\tau_e}{s} - \frac{|x_e|}{\|\mathbf{x}\|}\right)\right) + q_e \left(\frac{1}{s^2} + \frac{1}{s} \left(\frac{\tau_e}{s} - \frac{|x_e|}{\|\mathbf{x}\|}\right)\right) + \left(\frac{\tau_e}{s} - \frac{|x_e|}{\|\mathbf{x}\|}\right)^2\right], \tag{5}
 \end{aligned}$$

where

$$\begin{aligned}
 &q_e \left(\frac{1}{s^2} + \frac{1}{s} \left(\frac{\tau_e}{s} - \frac{|x_e|}{\|\mathbf{x}\|}\right)\right) \\
 &= \left(\frac{|x_e|}{\|\mathbf{x}\|}s - \tau_e\right) \left(\frac{1}{s^2} + \frac{1}{s} \left(\frac{\tau_e}{s} - \frac{|x_e|}{\|\mathbf{x}\|}\right)\right) \\
 &= -s \left(\frac{\tau_e}{s} - \frac{|x_e|}{\|\mathbf{x}\|}\right) \frac{1}{s} \left(\frac{1}{s} + \left(\frac{\tau_e}{s} - \frac{|x_e|}{\|\mathbf{x}\|}\right)\right) \\
 &= -\left(\frac{\tau_e}{s} - \frac{|x_e|}{\|\mathbf{x}\|}\right)^2 - \frac{1}{s} \left(\frac{\tau_e}{s} - \frac{|x_e|}{\|\mathbf{x}\|}\right).
 \end{aligned}$$

Substituting the result in (5), obtain

$$\begin{aligned}
 \mathbb{E}[\|\mathcal{C}_{\text{mrc}}(\mathbf{x}) - \mathbf{x}\|^2] &= \mathbb{E}\left[\sum_{e=1}^d (\mathcal{C}_{\text{mrc}}(x_e) - x_e)^2\right] \\
 &= \|\mathbf{x}\|^2 \sum_{e=1}^d \left[(\tilde{q}_e - q_e) \left(\frac{1}{s^2} + \frac{1}{s} \left(\frac{\tau_e}{s} - \frac{|x_e|}{\|\mathbf{x}\|}\right)\right) - \frac{1}{s} \left(\frac{\tau_e}{s} - \frac{|x_e|}{\|\mathbf{x}\|}\right)\right] \\
 &= \|\mathbf{x}\|^2 \sum_{e=1}^d \left[(\tilde{q}_e - q_e) \frac{1}{s} \left(\frac{\tau_e + 1}{s} - \frac{|x_e|}{\|\mathbf{x}\|}\right) - \frac{1}{s} \left(\frac{\tau_e}{s} - \frac{|x_e|}{\|\mathbf{x}\|}\right)\right] \\
 &\leq \|\mathbf{x}\|^2 \sum_{e=1}^d \left[|\tilde{q}_e - q_e| \frac{1}{s} \left(\frac{\tau_e + 1}{s} - \frac{|x_e|}{\|\mathbf{x}\|}\right) + \frac{1}{s} \left(\frac{|x_e|}{\|\mathbf{x}\|} - \frac{\tau_e}{s}\right)\right] \\
 &\leq \|\mathbf{x}\|^2 (|\tilde{q}_e - q_e| \frac{d}{s^2} + \frac{d}{s^2}),
 \end{aligned}$$

where, by Lemma 2, we have for $\Delta_e := \frac{q_e}{p_e} - \frac{1-q_e}{1-p_e}$ and $\Delta'_e := q_e \left(\frac{p_e}{q_e} + \frac{1-p_e}{1-q_e} \right)$ that

$$|\tilde{q}_e - q_e| \leq \frac{\Delta'_e}{n_{\text{IS}}^2} + \mathcal{O} \left((\Delta_e + \Delta_e^2) \sqrt{\frac{6p_e \log(2n_{\text{IS}})}{n_{\text{IS}}}} \right).$$

Let $\bar{\Delta} := \max_{e \in [d]} \frac{q_e}{p_e} - \frac{1-q_e}{1-p_e}$, $\bar{\Delta}' := \max_{e \in [d]} q_e \left(\frac{p_e}{q_e} + \frac{1-p_e}{1-q_e} \right)$, and $\bar{p} := \max_{e \in [d]} p_e$. We will ensure that $\frac{\bar{\Delta}'}{n_{\text{IS}}^2} + \mathcal{O} \left((\bar{\Delta} + \bar{\Delta}^2) \sqrt{\frac{6\bar{p} \log(2n_{\text{IS}})}{n_{\text{IS}}}} \right) \leq 1$ by making each of the individual terms $\leq \frac{1}{2}$. By choosing $n_{\text{IS}} \geq \sqrt{2\bar{\Delta}'}$, we have $\frac{\bar{\Delta}'}{n_{\text{IS}}^2} \leq \frac{1}{2}$. To ensure that $(\bar{\Delta} + \bar{\Delta}^2) \sqrt{\frac{6\bar{p} \log(2n_{\text{IS}})}{n_{\text{IS}}}} \leq \frac{1}{2}$, we require $\frac{\log(2n_{\text{IS}})}{n_{\text{IS}}} \leq \frac{1}{\sqrt{6\bar{p}(\bar{\Delta} + \bar{\Delta}^2)}}$. By Weinberger & Yemini (2023, Lemma 15), this holds when $n_{\text{IS}} = \mathcal{O}(\log(6\bar{p}(\bar{\Delta} + \bar{\Delta}^2))\sqrt{6\bar{p}(\bar{\Delta} + \bar{\Delta}^2)})$. Hence, choosing $n_{\text{IS}} = \mathcal{O}(\max\{\sqrt{2\bar{\Delta}'}, \log(6\bar{p}(\bar{\Delta} + \bar{\Delta}^2))\sqrt{6\bar{p}(\bar{\Delta} + \bar{\Delta}^2)}\})$, we have $\frac{\bar{\Delta}'}{n_{\text{IS}}^2} + \mathcal{O} \left((\bar{\Delta} + \bar{\Delta}^2) \sqrt{\frac{6\bar{p} \log(2n_{\text{IS}})}{n_{\text{IS}}}} \right) \leq 1$. Thus, we have $0 \leq \delta \leq 1$ if $\frac{2^d}{s^2} \leq 1$, and hence $s \geq \sqrt{2d}$. This concludes the proof. \square

Proof of Theorem 1. Assume a party estimates the Bernoulli distributions Q_j with parameters q_j held by parties $j \in [n]$. The estimating party shares with each of the other parties a common prior P_j in the form of a Bernoulli distribution with parameter p_j and access to unlimited shared randomness. To help estimate Q_j , the j -th party sends K samples to the estimator through MRC. Therefore, both parties sample Kn_{IS} i.i.d. samples $X_{\ell,i} \sim P_j$ for $\ell \in [K], i \in [n_{\text{IS}}]$, independently and identically from P_j . The party holding Q_j constructs for each $\ell \in [K]$ an auxiliary distribution

$$W_\ell(i) = \frac{Q_j(X_{\ell,i})/P_j(X_{\ell,i})}{\sum_{i=1}^{n_{\text{IS}}} Q_j(X_{\ell,i})/P_j(X_{\ell,i})},$$

from which it samples to obtain an index I_ℓ . The index is transmitted to the estimating party, which reconstructs the corresponding sample X_{ℓ,I_ℓ} . Averaging the samples for all $\ell \in [K]$ gives an estimate \hat{q}_j of q_j , i.e., $\hat{q}_j = \frac{1}{K} \sum_{\ell=1}^K X_{\ell,I_\ell}$. This process is repeated for all $j \in [n]$.

We assume that $|q_j - p_j| \leq \rho$ for all $i, j \in [n]$, and that the difference between the priors, is bounded as $|p_i - p_j| \leq \zeta$ for all $i, j \in [n]$. The goal is to bound $\text{d}_{\text{KL}} \left(\frac{1}{n} \sum_{j=1}^n \hat{q}_j \| p_i \right)$ from above for any $i \in [n]$.

By the convexity of KL-divergence, we have

$$\text{d}_{\text{KL}} \left(\frac{1}{n} \sum_{j=1}^n \hat{q}_j \| p_i \right) \leq \frac{1}{n} \sum_{i=1}^n \text{d}_{\text{KL}}(\hat{q}_j \| p_i).$$

To bound $\text{d}_{\text{KL}}(\hat{q}_j \| p_i)$ for any $i, j \in [n]$, by the triangle inequality, we can write

$$|\hat{q}_j - p_i| \leq |\hat{q}_j - \Pr(X_\ell = 1)| + |\Pr(X_\ell = 1) - q_j| + |q_j - p_j| + |p_j - p_i|,$$

where $|\hat{q}_j - \Pr(X_\ell = 1)|$ is bounded by Lemma 2. By Hoeffding's inequality, we have with probability at least $1 - \delta'$ that

$$|\hat{q}_j - \Pr(X_\ell = 1)| \leq \sqrt{\frac{-\ln(\delta'/2)}{2n_{\text{IS}}}}.$$

Thus, with probability at least $1 - \delta'$, since $p_j \leq p_i + \zeta$, we have with $\Delta_j := \frac{q_j}{p_j - \zeta} - \frac{1-q_j}{1-p_j + \zeta}$ and $\Delta'_j := q_j \left(\frac{p_j + \zeta}{q_j} + \frac{1-p_j + \zeta}{1-q_j} \right)$ that

$$|\hat{q}_j - p_i| \leq \frac{\Delta'_j}{n_{\text{IS}}^2} + \mathcal{O} \left((\Delta_j + \Delta_j^2) \sqrt{\frac{6(p_i + \zeta) \log(2n_{\text{IS}})}{n_{\text{IS}}}} \right) + \sqrt{\frac{-\ln(\delta'/2)}{2n_{\text{IS}}}} + \rho + \zeta.$$

This holds under the assumption that $p_j > \zeta$ for all $j \in [n]$. By the reversed Pinsker's inequality, we obtain

$$\begin{aligned} D_{\text{KL}}(\hat{q}_j \| p_i) \leq & \frac{2}{\min\{p_i, 1 - p_i\}} \left(\frac{\Delta'_j}{n_{\text{IS}}^2} + \mathcal{O} \left((\Delta_j + \Delta_j^2) \sqrt{\frac{6(p_i + \zeta) \log(2n_{\text{IS}})}{n_{\text{IS}}}} \right) \right. \\ & \left. + \sqrt{\frac{-\ln(\delta'/2)}{2n_{\text{IS}}}} + \rho + \zeta \right)^2. \end{aligned}$$

The statement of the theorem follows by the convexity of KL-divergence. \square

C Convergence Analysis

Using the contraction property derived in Lemma 1, we can show that a straightforward extension of BiCompFL-GR-CFL to error-feedback as used in (Richtárik et al., 2021) leads to the following convergence guarantee. Therefore, assume that for all $\mathbf{x}, \mathbf{y} \in \mathbb{R}^d$ and $i \in [n]$, the following Lipschitz property holds:

$$\|\nabla F(\mathbf{x}, \mathcal{D}_i) - \nabla F(\mathbf{y}, \mathcal{D}_i)\| \leq L_i \|\mathbf{x} - \mathbf{y}\|$$

Let $F(\theta) := \frac{1}{n} \sum_{i=1}^n \nabla F(\theta, \mathcal{D}_i)$ be the global loss function and $L' := \sqrt{\frac{1}{n} \sum_{i=1}^n L_i}$.

Theorem 2. *If $F^* := \inf_{\theta \in \mathbb{R}^d} \{F(\theta)\} > -\infty$ and $\mathbb{E}[\|\mathbf{g}^t - \nabla F(\theta_t)\|^2] \leq \sigma^2$, then with $\eta \leq \left(L + L' \sqrt{\frac{1-\delta}{(1-\sqrt{1-\delta})^2}}\right)^{-1}$, $L = 1$, $s \geq \sqrt{2d}$, and n_{IS} satisfying Lemma 1 in every iteration t , we have for a straightforward extension of BiCompFL-GR-CFL to error-feedback such that*

$$\sum_{t=1}^T \mathbb{E} [\|F(\theta_t)\|^2] \leq \frac{2(F(\theta_0) - F^*)}{\eta T} + \frac{\sigma^2}{(1 - \sqrt{1 - \delta})T}.$$

Similarly, guarantees can be derived for other algorithms, such as modified versions of BiCompFL-PR with error-feedback and momentum, using Lemma 1. However, we emphasize the generality of BiCompFL, reaching beyond conventional FL with stochastic compression to pure stochastic narratives.

D Gradient Descent with a KL-Proximity

Mirror descent employs point-wise optimization in the form of a first-order approximation of $F(\hat{\theta}_t, \mathcal{D}_i)$ with proximity term $D_F(p, q)$, where D_F is the Bregman divergence associated with function $F(\cdot)$. When $F(x) = \|x\|^2$, and hence the Bregman divergence is the Euclidean distance, this is known as gradient descent. Let now p and q be vectors with the entries corresponding to independent Bernoulli parameters. When we choose $F(x) = x \log(x) + (1-x) \log(1-x)$, the Bregman divergence becomes $D_F(p, q) = \sum_{k=1}^d D_{\text{KL}}(p_k \| q_k)$. Hence, we are optimizing with respect to a KL-proximity constraint. The mapping between dual and primal spaces is then given by $\nabla F(x) = \log(x) - \log(1-x)$ and $(\nabla F(x))^{-1} = \frac{1}{e^{-x} + 1}$, respectively; also known as the inverse sigmoid and the sigmoid functions.

E Block Allocation

The simplest yet effective strategy for block allocation is to partition the model into equally-sized blocks of size d/B for MRC (Fixed). The partitioning into blocks is required to make MRC practically feasible in this setting. It is known that for vanishing MRC error, the number of samples n_{IS} from a block $p_{i,u,b}^t$ of the prior is supposed to be in the order of $\exp\left(D_{\text{KL}}\left(q_{i,b}^t \| p_{i,u,b}^t\right)\right)$, where $q_{i,b}^t$ is the b -th block of posterior q_i^t . It was observed by (Isik et al., 2024) that the KL-divergence decreases as the training progresses with the global model used as a prior, which is intuitive since the local training will change the posterior less and less as training converges. To adapt the block size according to the divergence from the posterior with respect to the prior, (Isik et al., 2024) proposed an adaptive block allocation strategy (Adaptive), where upon realizing a large deviation from the target KL-divergence per block, clients partition their model

into blocks with equal sums of parameter-wise KL-divergences and transmit the block intervals to the federator. The federator aggregates the indices of all the clients, and broadcasts the updated block allocation. We propose in this work a low complexity solution that adapts the block size according to the average KL-divergence per block (Adaptive-Avg). This alleviates the cost of computing and transmitting the exact block partitions, where the transmission of each block size requires $\log_2(b_{\max})$ bits, with b_{\max} the maximum pre-defined block size. Instead, the transmission of one size is enough in our solution. If the average KL per block $D_{\text{KL}}(q_{i,b}^t \| p_{i,u,b}^t)$ deviates more than a given factor, the clients request to update the blocks. In the next iteration, each client proposes a block size, and the federator averages and broadcasts an updated size.

F Additional Experimental Details

We use the cross-entropy loss and a batch size of 128 in all our experiments. We use Adam (Kingma & Ba, 2015) as an optimizer with learning rate $\eta = 0.0003$ for all non-stochastic methods, and $\eta = 0.1$ for probabilistic mask training. For non-stochastic FL, we use a federator (server) learning rate of 0.1, i.e., the clients’ gradients are averaged, and the federator updates the global model with learning rate 0.1, and with a learning rate of 0.005 for BiCOMPFL-GR with SignSGD. For M3, we use a federator learning rate of 0.02 to obtain reliable results. For LIEC and CSER, we use an average period of 50 global iterations (cf. (Cheng et al., 2024; Xie et al., 2020)). For M3, we use TopK with $K = \lfloor d/n \rfloor$. To run the simulations, we use a cluster of different architectures, which we list in the following table.

| CPU(s) | RAM | GPU(s) | VRAM |
|--|--------|-------------------------------|-------|
| 2x Intel Xeon Platinum 8176 (56 cores) | 256 GB | 2x NVIDIA GeForce GTX 1080 Ti | 11 GB |
| 2x AMD EPYC 7282 (32 cores) | 512 GB | NVIDIA GeForce RTX 4090 | 24 GB |
| 2x AMD EPYC 7282 (32 cores) | 640 GB | NVIDIA GeForce RTX 4090 | 24 GB |
| 2x AMD EPYC 7282 (32 cores) | 448 GB | NVIDIA GeForce RTX 4080 | 16 GB |
| 2x AMD EPYC 7282 (32 cores) | 256 GB | NVIDIA GeForce RTX 4080 | 16 GB |
| HGX-A100 (96 cores) | 1 TB | 4x NVIDIA A100 | 80 GB |
| DGX-A100 (252 cores) | 2 TB | 8x NVIDIA Tesla A100 | 80 GB |
| DGX-1-V100 (76 cores) | 512 GB | 8x NVIDIA Tesla V100 | 16 GB |
| DGX-1-P100 (76 cores) | 512 GB | 8x NVIDIA Tesla P100 | 16 GB |
| HPE-P100 (28 cores) | 256 GB | 4x NVIDIA Tesla P100 | 16 GB |

Table 1: System specifications of our simulation cluster.

The details of the CNN architectures used in our experiments are summarized in the following. The parameter count is 61706 for LeNet5, 1933258 for 4CNN, and 2262602 for 6CNN.

Table 2: LeNet5 Architecture Overview

| Layer | Specification | Activation |
|----------|----------------------|---------------------|
| 5x5 Conv | 6 filters, stride 1 | ReLU, AvgPool (2x2) |
| 5x5 Conv | 16 filters, stride 1 | ReLU, AvgPool (2x2) |
| Linear | 120 units | ReLU |
| Linear | 84 units | ReLU |
| Linear | 10 units | Softmax |

Table 3: 4-layer CNN (4CNN) Architecture Overview

| Layer | Specification | Activation |
|----------|-----------------------|---------------------|
| 3x3 Conv | 64 filters, stride 1 | ReLU |
| 3x3 Conv | 64 filters, stride 1 | ReLU, MaxPool (2x2) |
| 3x3 Conv | 128 filters, stride 1 | ReLU |
| 3x3 Conv | 128 filters, stride 1 | ReLU, MaxPool (2x2) |
| Linear | 256 units | ReLU |
| Linear | 256 units | ReLU |
| Linear | 10 units | Softmax |

Table 4: 6-layer CNN (6CNN) Architecture Overview

| Layer | Specification | Activation |
|----------|-----------------------|---------------------|
| 3x3 Conv | 64 filters, stride 1 | ReLU |
| 3x3 Conv | 64 filters, stride 1 | ReLU, MaxPool (2x2) |
| 3x3 Conv | 128 filters, stride 1 | ReLU |
| 3x3 Conv | 128 filters, stride 1 | ReLU, MaxPool (2x2) |
| 3x3 Conv | 256 filters, stride 1 | ReLU |
| 3x3 Conv | 256 filters, stride 1 | ReLU, MaxPool (2x2) |
| Linear | 256 units | ReLU |
| Linear | 256 units | ReLU |
| Linear | 10 units | Softmax |

For the sake of clarity, in the paper we restrict the analysis to a fixed number of importance samples n_{IS} , block sizes B , and choice of priors $p_{i,u}^t, p_{i,d}^t$. Our experiments have shown that, while increasing n_{IS} beyond the ones used in our algorithms slightly improves the convergence over the number of epochs, the convergence with respect to the communication cost did not significantly improve. The block size is mainly limited by the system resources at hand, and one would choose the largest possible for best efficiency while complying with memory resources. We investigated many different prior choices and found the former global model to be reasonably good in almost all cases. With high heterogeneity, it might be beneficial to use different convex combinations as priors, which mix the former global model with the latest posterior estimate of a certain client, but the gains we experienced were minor. Hence, we settled on the former global estimate for simplicity in presenting the algorithm.

G Federated Probabilistic Mask Training

The idea in federated probabilistic mask training (FedPM) (Isik et al., 2023) is to collaboratively train a probabilistic mask that determines which weights to maintain from a randomly initialized network. The motivation stems from the *lottery-ticket hypothesis* (Frankle & Carbin, 2019), which claims that randomly initialized networks contain sub-networks capable of reaching accuracy comparable to that of the full network. The weights w of the network are randomly initialized at the start of training, and remain fixed. The federator and clients only train a mask, which determines for each parameter whether it is activated or not, i.e., identifying an efficient subnetwork within the given fixed network. The probabilistic masks θ_t are described by Bernoulli distributions, i.e., $\theta_t \in [0, 1]^d$ contains a Bernoulli parameter to be trained for each weight of the network. These parameters determine the probability of retaining the corresponding weights. During inference, the weights w are masked with samples $x^t \in \{0, 1\}^d \sim \theta_t$ from the distribution θ_t , i.e., the inference is conducted on a network with weights $w \odot x^t$. In FedPM, clients sample from their locally trained models, and send these samples to the federator, which, in turn, updates the global model by averaging these samples. The communication cost of this scheme is fixed for all iterations, even though the communication cost can be reduced since the KL-divergence between the global model and the locally trained models diminishes as the training progresses.

We adopt the following federated learning procedure for collaboratively learning network masks, and highlight in the following the parallels to mirror descent by referring to primal and dual spaces. Starting from a common model θ_0 , at

Algorithm 3 Local Training at Client i

Require: Model $\hat{\theta}_{i,t}$

- 1: Map model to scores in the dual space: $\mathbf{s}_{i,t}^{(0)} = \sigma^{-1}(\hat{\theta}_{i,t}) = \log\left(\frac{\hat{\theta}_{i,t}}{1-\hat{\theta}_{i,t}}\right)$
 - 2: **for** Local iterations $m \in [L]$ **do**
 - 3: $\mathbf{s}_{i,t}^{(\ell)} = \mathbf{s}_{i,t}^{(0)} - \eta \nabla_{\mathbf{s}_{i,t}^{(\ell-1)}} F(\hat{\theta}_{i,t}^{(m-1)}, \mathcal{D}_i)$, where $\hat{\theta}_{i,t}^{(m-1)} = \sigma(\mathbf{s}_{i,t}^{(\ell-1)})$
 - 4: **end for**
 - 5: Map back to primal space: $q_i^t = \sigma(\mathbf{s}_{i,t}^{(L)})$
-

iteration t , each client i locally trains the model $\hat{\theta}_{i,t}$ in L local iterations. To enable gradient descent, the model $\hat{\theta}_{i,t}$ is mapped to scores $\mathbf{s}_{i,t}^{(0)}$ in a dual space by the inverse Sigmoid function $\mathbf{s}_{i,t}^{(0)} = \sigma^{-1}(\hat{\theta}_{i,t}) = \log(\hat{\theta}_{i,t}) - \log(1 - \hat{\theta}_{i,t})$. The scores are then trained for L local iterations $m \in [L]$ by computing the gradient $\nabla_{\mathbf{s}_{i,t}^{(\ell-1)}} F(\hat{\theta}_{i,t}^{(m-1)}, \mathcal{D}_i)$, where the straight-through estimator is used to compute the gradient of the non-differentiable Bernoulli sampling operation based on the distribution $\hat{\theta}_{i,t}^{(m-1)} = \sigma(\mathbf{s}_{i,t}^{(\ell-1)})$, i.e., the gradient equals the Bernoulli parameter. By mapping the model back to the primal space, each client i obtains a model update in terms of a posterior $q_i^t = \sigma(\mathbf{s}_{i,t}^{(L)})$. The client training process is summarized in Algorithm 3.

H Minimal Random Coding (MRC)

Isik et al. (2024) proposed a method, called KL minimization with side information (KLMS), to reduce the cost of transmitting the local models q_i^t to the federator. Consequently, the communication cost depends on the KL-divergence between the desired distribution and the common prior. This method utilizes the common side information available at both the clients and the federator, as well as shared randomness. The idea is that instead of sampling locally and sending the samples to the federator, the federator in the KLMS method samples from the desired distribution through MRC. In a nutshell, MRC (Havasi et al., 2019) is based on importance sampling (Srinivasan, 2002) and makes use of a common prior to sample from a desired distribution. Consider two distributions P and Q , where P is known to both parties, and Q is only known to the client. To make the federator sample from Q , both parties sample n_{IS} samples $\{X_i\}_{i \in [n_{\text{IS}}]}$ from P . The client forms an auxiliary distribution $W(i) = \frac{Q(X_i)/P(X_i)}{\sum_{i=1}^{n_{\text{IS}}} Q(X_i)/P(X_i)}$ capturing the importance of the samples. A sample from W is fully described by its index i , which can be transmitted with $\log_2(n_{\text{IS}})$ bits, and approximates a sample from Q . Chatterjee & Diaconis (2018) shown that importance sampling with posterior Q and prior P requires n_{IS} to be in the order of $\Theta(\exp(\text{D}_{\text{KL}}(Q\|P)))$, where $\text{D}_{\text{KL}}(Q\|P)$ denotes the KL-divergence between distributions Q and P . In what follows, we will also denote the KL-divergence between two Bernoulli distributions Q and P with parameters q and p by $\text{d}_{\text{KL}}(q\|p)$.

I Additional Experiments

We provide in the following experiments for both uniform (i.i.d.) and heterogeneous (non-i.i.d.) data distributions for training LeNet5 and a 4-layer CNN on MNIST, a 4-layer CNN on Fashion MNIST, and a 6-layer CNN on CIFAR-10. The details of the neural networks can be found in Tables 2 to 4. For each setting and method depicted, we show the average of three simulation runs with different seeds. We plot for each setting the test accuracies over the communication cost in bits, and the maximum test accuracy over the bitrate. We provide tables summarizing the maximum test accuracies with their standard deviation over multiple runs, the total bitrates and the bitrates split into uplink and downlink. The overall bitrates per parameter (bpp) are computed assuming point-to-point links between all participants, i.e., uplink and downlink costs have equal weight. For the case when a broadcast (BC) link between the federator and the clients is available, the bitrate per parameter for all baseline schemes reduces by a factor of n . BiCompFL-GR profits similarly from the broadcast link, but BiCompFL-PR cannot profit due to the absence of shared randomness, giving the same overall bitrate compared to the point-to-point link scenario. We highlight for each of the measures the scheme with the best result. Consistently throughout all experiments, BiCompFL achieves order-wise savings in the bitrates per parameter while reaching state-of-the-art accuracies in the classification task. While the sampling can introduce an additional computational overhead depending on the implementation, the storage cost is similar to the baselines. Since we leverage as priors the former global model, the additional storage cost incurred is limited to storing until the next iteration the estimate of the former global model at each client, i.e., where the training started, which is usually not a bottleneck. This can be cheaper than some

baselines, which require storing data for momentum and error-feedback.

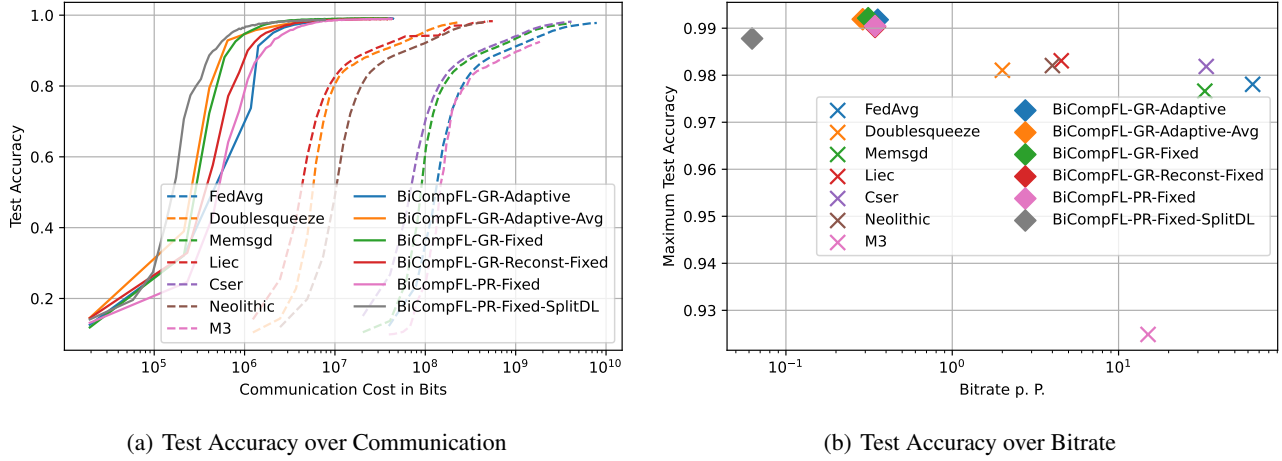


Figure 3: MNIST LeNet i.i.d.

For LeNet5 on MNIST, it can be observed that all our proposed methods converge significantly faster to satisfying accuracies with respect to the communication cost, while achieving higher maximum accuracies after 200 epochs than the non-stochastic baselines. Partitioning the model on the downlink can help to further reduce the communication cost with only a minor loss in performance, especially in the i.i.d. setting. For non-i.i.d. data distribution, the loss in performance is larger than for i.i.d. distribution. However, at the beginning of the training, the model improves faster with respect to the communication cost than all other schemes. The bitrates are comparable for all our methods, with the exception of BiCompFL-PR-Fixed-SplitDL. Further, BiCompFL-GR-Reconst-Fixed does not suffer notable performance degradation from employing an additional MRC step (especially for i.i.d. data allocation).

Table 5: MNIST LeNet i.i.d.

| Method | Acc (mean \pm std) | bpp | bpp (BC) | Uplink | Downlink |
|---------------------------|--------------------------------------|--------------|--------------|--------------|--------------|
| FedAvg | 0.978 \pm 0.1 | 64.0 | 35.0 | 32.0 | 32.0 |
| Doublesqueeze | 0.981 \pm 0.1 | 2.0 | 1.1 | 1.0 | 1.0 |
| Memsgd | 0.977 \pm 0.1 | 33.0 | 4.2 | 1.0 | 32.0 |
| Liec | 0.983 \pm 0.1 | 4.5 | 2.5 | 2.3 | 2.3 |
| Cser | 0.982 \pm 0.09 | 34.0 | 4.3 | 1.0 | 33.0 |
| Neolithic | 0.982 \pm 0.1 | 4.0 | 2.2 | 2.0 | 2.0 |
| M3 | 0.925 \pm 0.2 | 15.0 | 2.2 | 8.0 | 7.1 |
| BiCompFL-GR-Adaptive | 0.992 \pm 0.0006 | 0.36 | 0.068 | 0.036 | 0.32 |
| BiCompFL-GR-Adaptive-Avg | 0.992 \pm 0.0003 | 0.29 | 0.055 | 0.029 | 0.26 |
| BiCompFL-GR-Fixed | 0.992 \pm 0.0002 | 0.31 | 0.059 | 0.031 | 0.28 |
| BiCompFL-GR-Reconst-Fixed | 0.99 \pm 0.0002 | 0.34 | 0.063 | 0.031 | 0.31 |
| BiCompFL-PR-Fixed | 0.99 \pm 0.0004 | 0.34 | 0.34 | 0.031 | 0.31 |
| BiCompFL-PR-Fixed-SplitDL | 0.988 \pm 0.0009 | 0.063 | 0.063 | 0.031 | 0.031 |

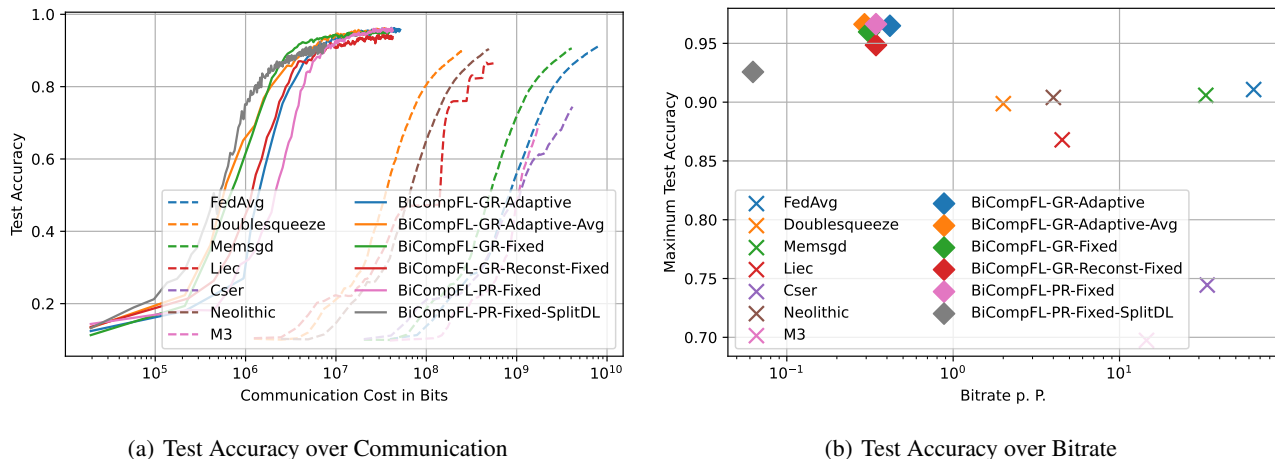


Figure 4: MNIST LeNet non-i.i.d.

Table 6: MNIST LeNet non-i.i.d.

| Method | Acc (mean \pm std) | bpp | bpp (BC) | Uplink | Downlink |
|---------------------------|------------------------------------|--------------|--------------|--------------|--------------|
| FedAvg | 0.911 \pm 0.2 | 64.0 | 35.0 | 32.0 | 32.0 |
| Doublesqueeze | 0.899 \pm 0.2 | 2.0 | 1.1 | 1.0 | 1.0 |
| Memsgd | 0.906 \pm 0.2 | 33.0 | 4.2 | 1.0 | 32.0 |
| Liec | 0.866 \pm 0.2 | 4.5 | 2.5 | 2.3 | 2.3 |
| Cser | 0.744 \pm 0.2 | 34.0 | 4.3 | 1.0 | 33.0 |
| Neolithic | 0.904 \pm 0.2 | 4.0 | 2.2 | 2.0 | 2.0 |
| M3 | 0.697 \pm 0.2 | 15.0 | 2.2 | 7.3 | 7.2 |
| BiCompFL-GR-Adaptive | 0.965 \pm 0.02 | 0.42 | 0.079 | 0.042 | 0.37 |
| BiCompFL-GR-Adaptive-Avg | 0.966 \pm 0.02 | 0.29 | 0.056 | 0.029 | 0.26 |
| BiCompFL-GR-Fixed | 0.96 \pm 0.03 | 0.31 | 0.059 | 0.031 | 0.28 |
| BiCompFL-GR-Reconst-Fixed | 0.949 \pm 0.03 | 0.34 | 0.063 | 0.031 | 0.31 |
| BiCompFL-PR-Fixed | 0.966 \pm 0.02 | 0.34 | 0.34 | 0.031 | 0.31 |
| BiCompFL-PR-Fixed-SplitDL | 0.926 \pm 0.04 | 0.063 | 0.063 | 0.031 | 0.031 |

For 4CNN trained on MNIST, the differences between the proposed approaches become more visible. In the i.i.d. setting, we can observe that the adaptive block allocations (both Adaptive and Adaptive-Avg) can drastically reduce the average bitrate in BiCompFL-GR. Partitioning the model in the downlink (BiCompFL-PR-Fixed-SplitDL) improves the accuracy over bitrate significantly compared to BiCompFL-PR-Fixed.

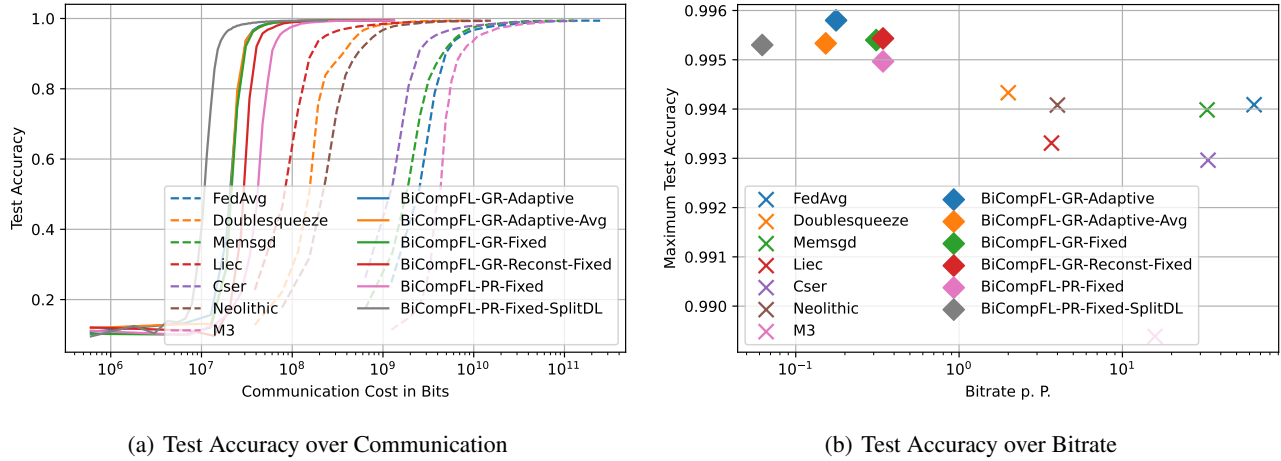


Figure 5: MNIST 4CNN i.i.d.

Table 7: MNIST 4CNN i.i.d.

| Method | Acc (mean \pm std) | bpp | bpp (BC) | Uplink | Downlink |
|---------------------------|--------------------------------------|--------------|--------------|--------------|--------------|
| FedAvg | 0.994 \pm 0.06 | 64.0 | 35.0 | 32.0 | 32.0 |
| Doublesqueeze | 0.994 \pm 0.1 | 2.0 | 1.1 | 1.0 | 1.0 |
| Memsgd | 0.994 \pm 0.08 | 33.0 | 4.2 | 1.0 | 32.0 |
| Liec | 0.993 \pm 0.07 | 3.7 | 2.0 | 1.8 | 1.8 |
| Cser | 0.993 \pm 0.06 | 33.0 | 4.3 | 1.0 | 32.0 |
| Neolithic | 0.994 \pm 0.08 | 4.0 | 2.2 | 2.0 | 2.0 |
| M3 | 0.989 \pm 0.2 | 16.0 | 2.2 | 8.4 | 7.4 |
| BiCompFL-GR-Adaptive | 0.996 \pm 0.0001 | 0.18 | 0.034 | 0.018 | 0.16 |
| BiCompFL-GR-Adaptive-Avg | 0.995 \pm 0.0001 | 0.15 | 0.029 | 0.015 | 0.14 |
| BiCompFL-GR-Fixed | 0.995 \pm 0.0002 | 0.31 | 0.059 | 0.031 | 0.28 |
| BiCompFL-GR-Reconst-Fixed | 0.995 \pm 0.0001 | 0.34 | 0.062 | 0.031 | 0.31 |
| BiCompFL-PR-Fixed | 0.995 \pm 0.0002 | 0.34 | 0.34 | 0.031 | 0.31 |
| BiCompFL-PR-Fixed-SplitDL | 0.995 \pm 0.0002 | 0.062 | 0.062 | 0.031 | 0.031 |

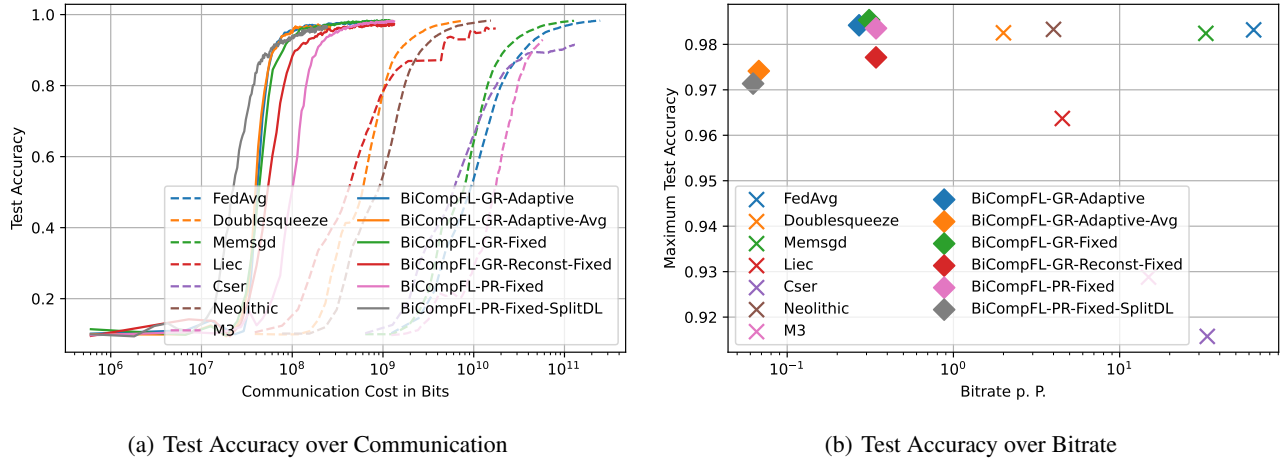


Figure 6: MNIST 4CNN non-i.i.d.

In the non-i.i.d. case of 4CNN on MNIST, the adaptive average allocation strategy provides a significant reduction in the bitrate for BiCompFL-GR, with similar loss in the accuracy as SplitDL for BiCompFL-PR. In this setting, it is also apparent that the reconstruction in BiCompFL-GR degrades the performance without gains in the bitrate compared to the proposed Algorithm 1.

Table 8: MNIST 4CNN non-i.i.d.

| Method | Acc (mean \pm std) | bpp | bpp (BC) | Uplink | Downlink |
|---------------------------|-------------------------------------|--------------|--------------|---------------|--------------|
| FedAvg | 0.983 \pm 0.1 | 64.0 | 35.0 | 32.0 | 32.0 |
| Doublesqueeze | 0.982 \pm 0.2 | 2.0 | 1.1 | 1.0 | 1.0 |
| Memsgd | 0.982 \pm 0.2 | 33.0 | 4.2 | 1.0 | 32.0 |
| Liec | 0.963 \pm 0.2 | 4.5 | 2.5 | 2.3 | 2.3 |
| Cser | 0.915 \pm 0.1 | 34.0 | 4.3 | 1.0 | 33.0 |
| Neolithic | 0.983 \pm 0.2 | 4.0 | 2.2 | 2.0 | 2.0 |
| M3 | 0.929 \pm 0.3 | 15.0 | 2.2 | 7.8 | 7.1 |
| BiCompFL-GR-Adaptive | 0.984 \pm 0.009 | 0.27 | 0.051 | 0.026 | 0.24 |
| BiCompFL-GR-Adaptive-Avg | 0.974 \pm 0.02 | 0.067 | 0.013 | 0.0068 | 0.061 |
| BiCompFL-GR-Fixed | 0.985 \pm 0.008 | 0.31 | 0.059 | 0.031 | 0.28 |
| BiCompFL-GR-Reconst-Fixed | 0.977 \pm 0.01 | 0.34 | 0.062 | 0.031 | 0.31 |
| BiCompFL-PR-Fixed | 0.984 \pm 0.009 | 0.34 | 0.34 | 0.031 | 0.31 |
| BiCompFL-PR-Fixed-SplitDL | 0.971 \pm 0.02 | 0.062 | 0.062 | 0.031 | 0.031 |

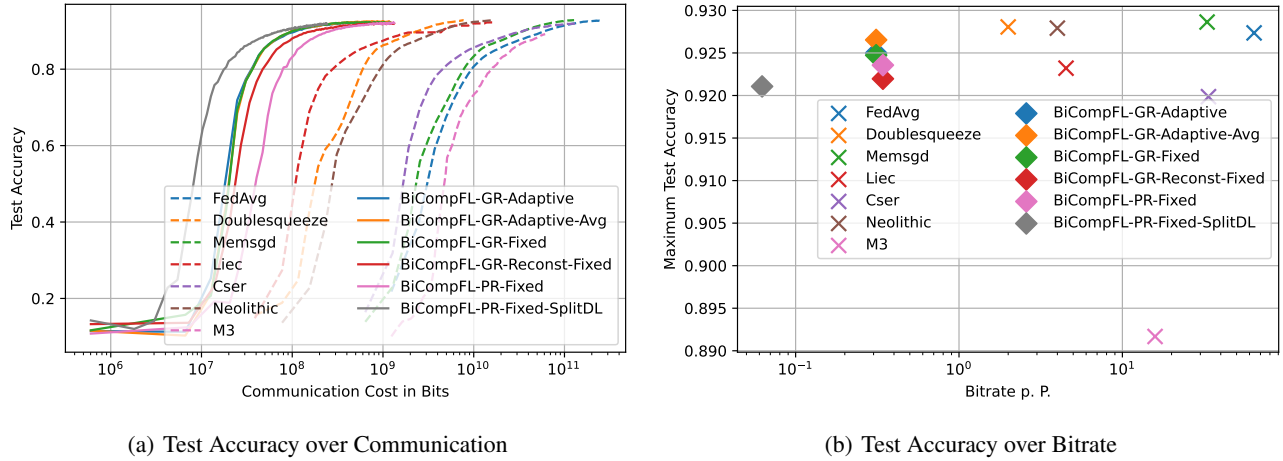


Figure 7: Fashion MNIST 4CNN i.i.d.

Table 9: Fashion MNIST 4CNN i.i.d.

| Method | Acc (mean \pm std) | bpp | bpp (BC) | Uplink | Downlink |
|---------------------------|-----------------------------------|--------------|--------------|--------------|--------------|
| FedAvg | 0.927 \pm 0.07 | 64.0 | 35.0 | 32.0 | 32.0 |
| Doublesqueeze | 0.928 \pm 0.1 | 2.0 | 1.1 | 1.0 | 1.0 |
| Memsgd | 0.928 \pm 0.09 | 33.0 | 4.2 | 1.0 | 32.0 |
| Liec | 0.923 \pm 0.08 | 4.5 | 2.5 | 2.3 | 2.3 |
| Cser | 0.92 \pm 0.08 | 34.0 | 4.3 | 1.0 | 33.0 |
| Neolithic | 0.928 \pm 0.09 | 4.0 | 2.2 | 2.0 | 2.0 |
| M3 | 0.892 \pm 0.2 | 16.0 | 2.2 | 8.3 | 7.6 |
| BiCompFL-GR-Adaptive | 0.925 \pm 0.001 | 0.31 | 0.059 | 0.031 | 0.28 |
| BiCompFL-GR-Adaptive-Avg | 0.927 \pm 0.0007 | 0.31 | 0.059 | 0.031 | 0.28 |
| BiCompFL-GR-Fixed | 0.925 \pm 0.0007 | 0.31 | 0.059 | 0.031 | 0.28 |
| BiCompFL-GR-Reconst-Fixed | 0.922 \pm 0.001 | 0.34 | 0.062 | 0.031 | 0.31 |
| BiCompFL-PR-Fixed | 0.924 \pm 0.002 | 0.34 | 0.34 | 0.031 | 0.31 |
| BiCompFL-PR-Fixed-SplitDL | 0.921 \pm 0.002 | 0.062 | 0.062 | 0.031 | 0.031 |

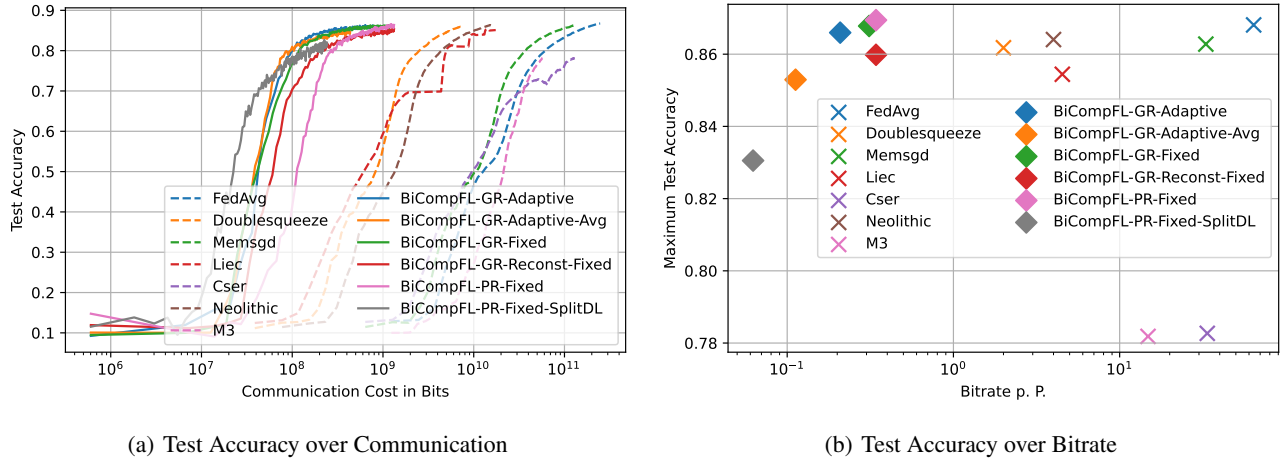


Figure 8: Fashion MNIST 4CNN non-i.i.d.

The results for Fashion MNIST are similar compared to the MNIST case. However, it becomes clear that BiCompFL-PR can significantly suffer from the unavailability of shared randomness in terms of the achieved accuracy when data is highly heterogeneous.

Table 10: Fashion MNIST 4CNN non-i.i.d.

| Method | Acc (mean \pm std) | bpp | bpp (BC) | Uplink | Downlink |
|---------------------------|------------------------------------|--------------|--------------|--------------|--------------|
| FedAvg | 0.867 \pm 0.1 | 64.0 | 35.0 | 32.0 | 32.0 |
| Doublesqueeze | 0.861 \pm 0.2 | 2.0 | 1.1 | 1.0 | 1.0 |
| Memsgd | 0.863 \pm 0.2 | 33.0 | 4.2 | 1.0 | 32.0 |
| Liec | 0.853 \pm 0.1 | 4.5 | 2.5 | 2.3 | 2.3 |
| Cser | 0.781 \pm 0.1 | 34.0 | 4.3 | 1.0 | 33.0 |
| Neolithic | 0.864 \pm 0.2 | 4.0 | 2.2 | 2.0 | 2.0 |
| M3 | 0.782 \pm 0.2 | 15.0 | 2.2 | 8.0 | 6.9 |
| BiCompFL-GR-Adaptive | 0.866 \pm 0.03 | 0.21 | 0.04 | 0.021 | 0.19 |
| BiCompFL-GR-Adaptive-Avg | 0.853 \pm 0.04 | 0.11 | 0.021 | 0.011 | 0.1 |
| BiCompFL-GR-Fixed | 0.868 \pm 0.03 | 0.31 | 0.059 | 0.031 | 0.28 |
| BiCompFL-GR-Reconst-Fixed | 0.86 \pm 0.02 | 0.34 | 0.062 | 0.031 | 0.31 |
| BiCompFL-PR-Fixed | 0.869 \pm 0.03 | 0.34 | 0.34 | 0.031 | 0.31 |
| BiCompFL-PR-Fixed-SplitDL | 0.831 \pm 0.03 | 0.062 | 0.062 | 0.031 | 0.031 |

For 6CNN trained on CIFAR-10, the negative effects of missing global shared randomness and reconstructing in the case of BiCompFL-GR are prominent. For non-i.i.d. data distributions, the adaptive average allocation shows improvements over the fixed or the average block allocation. Partitioning the model is not a viable option in this setting, especially under non-i.i.d. data.

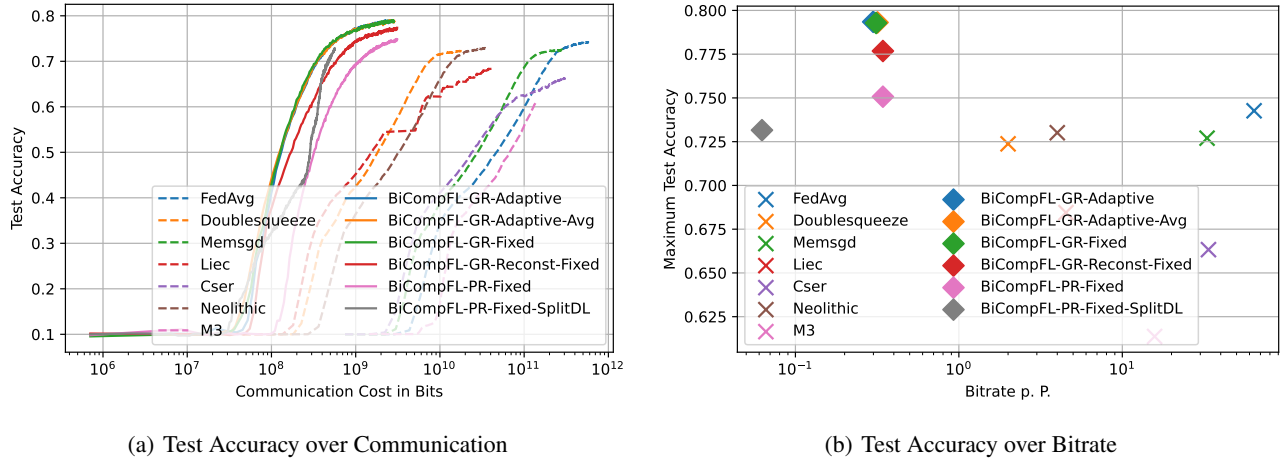


Figure 9: CIFAR-10 6CNN i.i.d.

Table 11: CIFAR-10 6CNN i.i.d.

| Method | Acc (mean \pm std) | bpp | bpp (BC) | Uplink | Downlink |
|---------------------------|-------------------------------------|--------------|--------------|-------------|--------------|
| FedAvg | 0.742 \pm 0.1 | 64.0 | 35.0 | 32.0 | 32.0 |
| Doublesqueeze | 0.723 \pm 0.1 | 2.0 | 1.1 | 1.0 | 1.0 |
| Memsgd | 0.727 \pm 0.1 | 33.0 | 4.2 | 1.0 | 32.0 |
| Liec | 0.684 \pm 0.09 | 4.5 | 2.5 | 2.3 | 2.3 |
| Cser | 0.663 \pm 0.08 | 34.0 | 4.3 | 1.0 | 33.0 |
| Neolithic | 0.73 \pm 0.1 | 4.0 | 2.2 | 2.0 | 2.0 |
| M3 | 0.614 \pm 0.1 | 16.0 | 2.2 | 8.3 | 7.5 |
| BiCompFL-GR-Adaptive | 0.793 \pm 0.002 | 0.3 | 0.057 | 0.03 | 0.27 |
| BiCompFL-GR-Adaptive-Avg | 0.793 \pm 0.002 | 0.32 | 0.061 | 0.032 | 0.29 |
| BiCompFL-GR-Fixed | 0.793 \pm 0.004 | 0.31 | 0.059 | 0.031 | 0.28 |
| BiCompFL-GR-Reconst-Fixed | 0.777 \pm 0.002 | 0.34 | 0.062 | 0.031 | 0.31 |
| BiCompFL-PR-Fixed | 0.751 \pm 0.003 | 0.34 | 0.34 | 0.031 | 0.31 |
| BiCompFL-PR-Fixed-SplitDL | 0.732 \pm 0.02 | 0.062 | 0.062 | 0.031 | 0.031 |

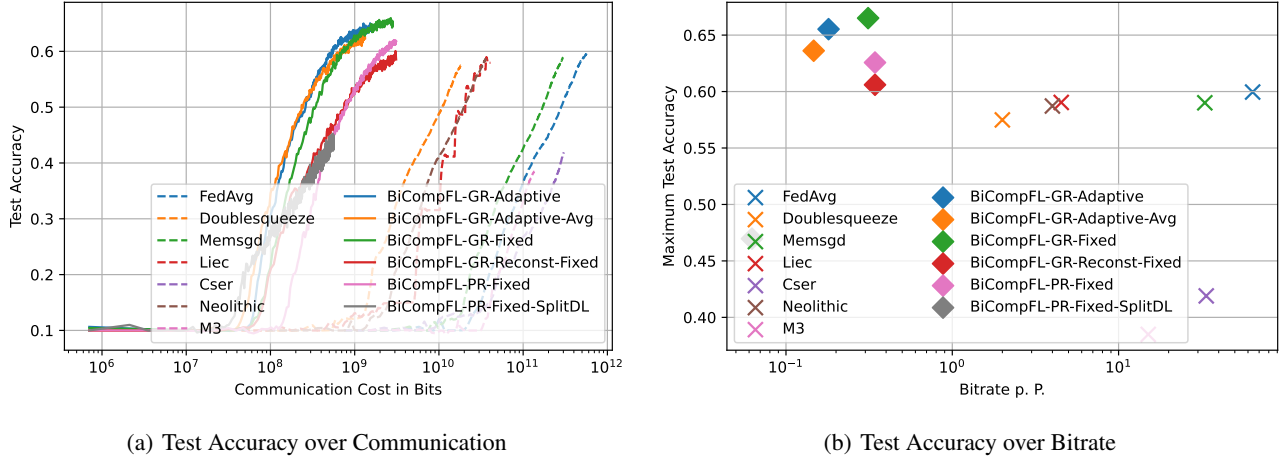


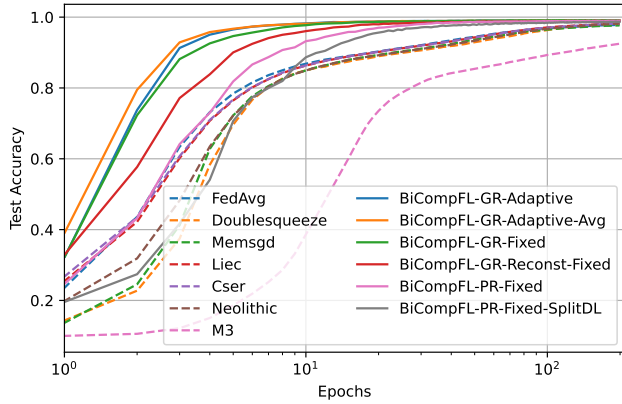
Figure 10: CIFAR-10 6CNN non-i.i.d.

Table 12: CIFAR-10 6CNN non-i.i.d.

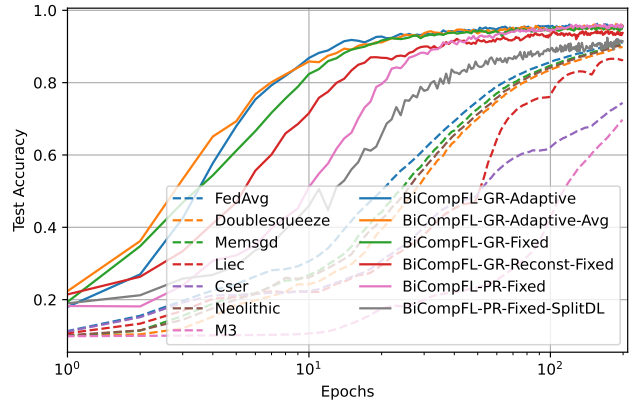
| Method | Acc (mean \pm std) | bpp | bpp (BC) | Uplink | Downlink |
|---------------------------|------------------------------------|--------------|--------------|--------------|--------------|
| FedAvg | 0.599 \pm 0.1 | 64.0 | 35.0 | 32.0 | 32.0 |
| Doublesqueeze | 0.575 \pm 0.1 | 2.0 | 1.1 | 1.0 | 1.0 |
| Memsgd | 0.589 \pm 0.1 | 33.0 | 4.2 | 1.0 | 32.0 |
| Liec | 0.589 \pm 0.2 | 4.5 | 2.5 | 2.3 | 2.3 |
| Cser | 0.419 \pm 0.09 | 34.0 | 4.3 | 1.0 | 33.0 |
| Neolithic | 0.587 \pm 0.1 | 4.0 | 2.2 | 2.0 | 2.0 |
| M3 | 0.385 \pm 0.1 | 15.0 | 2.2 | 8.3 | 6.7 |
| BiCompFL-GR-Adaptive | 0.655 \pm 0.04 | 0.18 | 0.034 | 0.018 | 0.16 |
| BiCompFL-GR-Adaptive-Avg | 0.636 \pm 0.05 | 0.15 | 0.028 | 0.015 | 0.13 |
| BiCompFL-GR-Fixed | 0.665 \pm 0.03 | 0.31 | 0.059 | 0.031 | 0.28 |
| BiCompFL-GR-Reconst-Fixed | 0.606 \pm 0.05 | 0.34 | 0.062 | 0.031 | 0.31 |
| BiCompFL-PR-Fixed | 0.626 \pm 0.03 | 0.34 | 0.34 | 0.031 | 0.31 |
| BiCompFL-PR-Fixed-SplitDL | 0.47 \pm 0.07 | 0.062 | 0.062 | 0.031 | 0.031 |

For completeness, we present in what follows the test accuracies over the number of trained epochs for all scenarios considered above. The setting of interest to this work is that of limited communication cost, and in particular, which performance is achievable given a fixed communication budget. Nonetheless, we can find that our proposed methods are not inferior in convergence speed over epochs compared to the baselines.

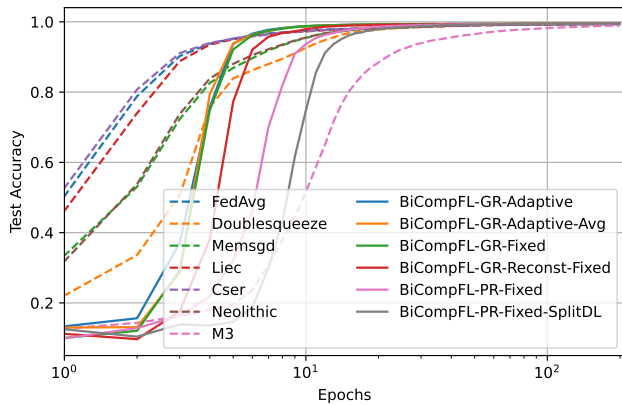
BiCompFL: Stochastic Federated Learning with Bi-Directional Compression



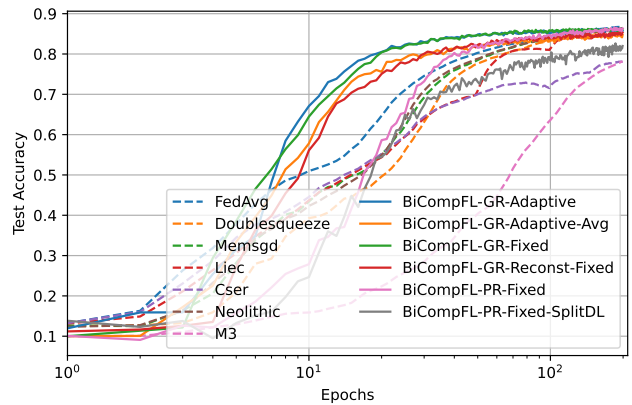
(a) MNIST LeNet i.i.d.



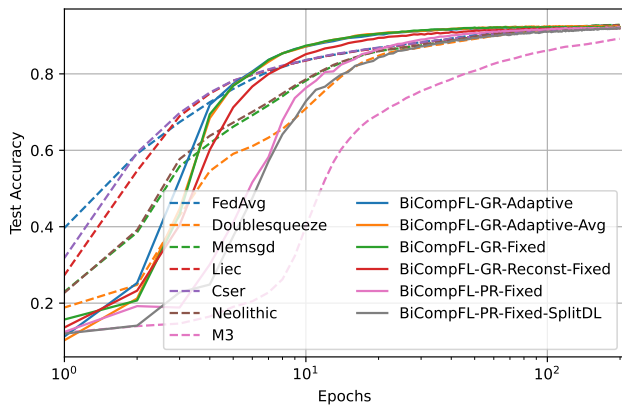
(b) MNIST LeNet non-i.i.d.



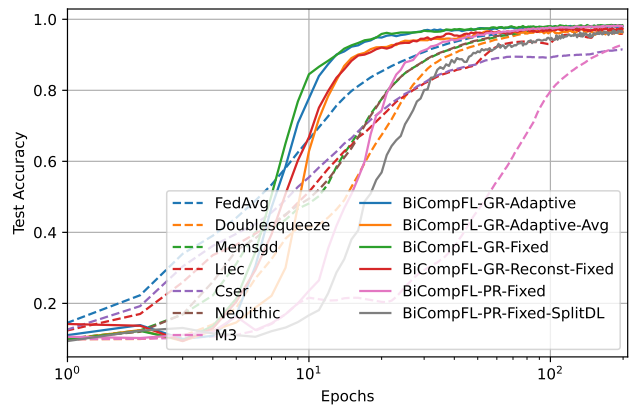
(c) MNIST 4CNN i.i.d.



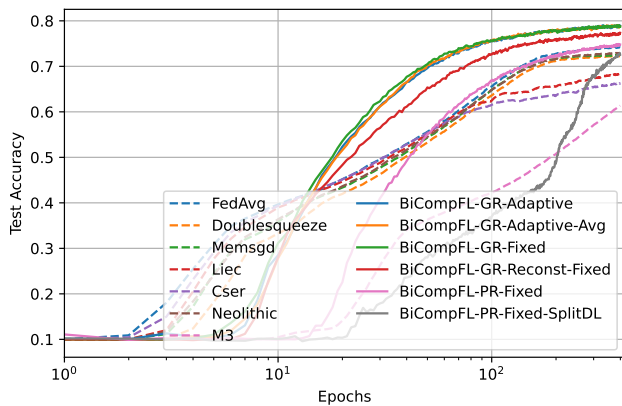
(d) MNIST 4CNN non-i.i.d.



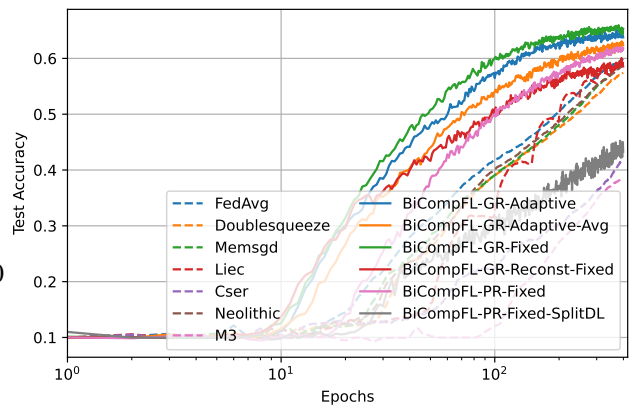
(e) Fashion MNIST 4CNN i.i.d.



(f) Fashion MNIST 4CNN non-i.i.d.



30



J Ablation Studies

J.1 Number of Clients

We study in what follows the sensitivity to various hyperparameters of our algorithms. For comparability, we conduct all experiments on the model 4CNN, Fashion MNIST, and i.i.d.data. We plot for all experiments the accuracies over the number of epochs, and over the communication cost in bits. We first evaluate in Fig. 12 the effectiveness of BiCompFL-GR and BiCompFL-PR for different numbers of clients. It can be found that both algorithms exhibit satisfying performance even for $n = 50$, given that the same data is now distributed on more clients. The overall communication cost increases by roughly the factor of the increase in the number of n . To illustrate this further, we additionally plot in Fig. 13 the bitrates per parameter.

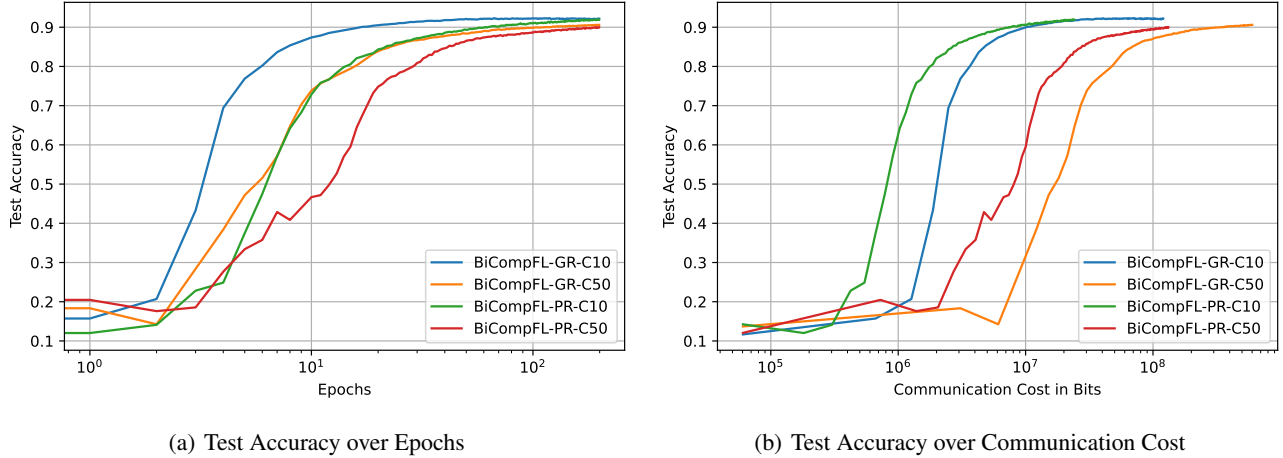


Figure 12: BiCompFL-GR and BiCompFL-GR With Different Number of Clients

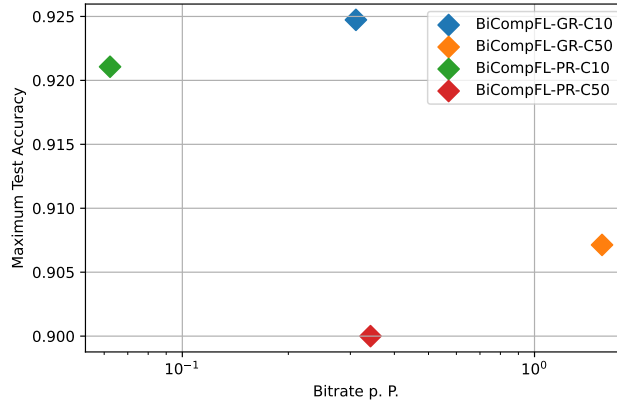


Figure 13: Bitrates for BiCompFL-GR and BiCompFL-GR With Different Number of Clients

J.2 Optimization of the Prior

As described in the main body of the paper, BiCompFL-PR allows for optimizing the choice of the prior at the clients by optimizing the convexity parameter λ that mixes the global model estimate with the posterior transmitted by the client an iteration ahead, i.e., $p_{i,u}^t = \lambda \hat{\theta}_{i,t} + (1 - \lambda) \hat{q}_i^t$ to reduce the communication cost. To evaluate the potential of this method, we optimize λ so that it minimized the KL-divergence between the current posterior q_i^t (to be transmitted) and the prior $p_{i,u}^t$,

representative for the uplink communication cost. The KL-minimizing λ is transmitted to the federator, which is necessary for the federator to reconstruct the importance samples. This optimization is conducted at each iteration individually at the clients. We present in Fig. 14 the performance of this method compared with the algorithms that use as priors exclusively the global model estimates of the clients. Note that optimizing the prior individually at the clients is only possible for BiCompFL-PR. We plot the performance of BiCompFL-GR for reference only. To assess the potential, we ignore for the moment the cost of transmitting λ , which could be reduced by further compression techniques and leveraging the inter-round dependencies of the choice of λ .

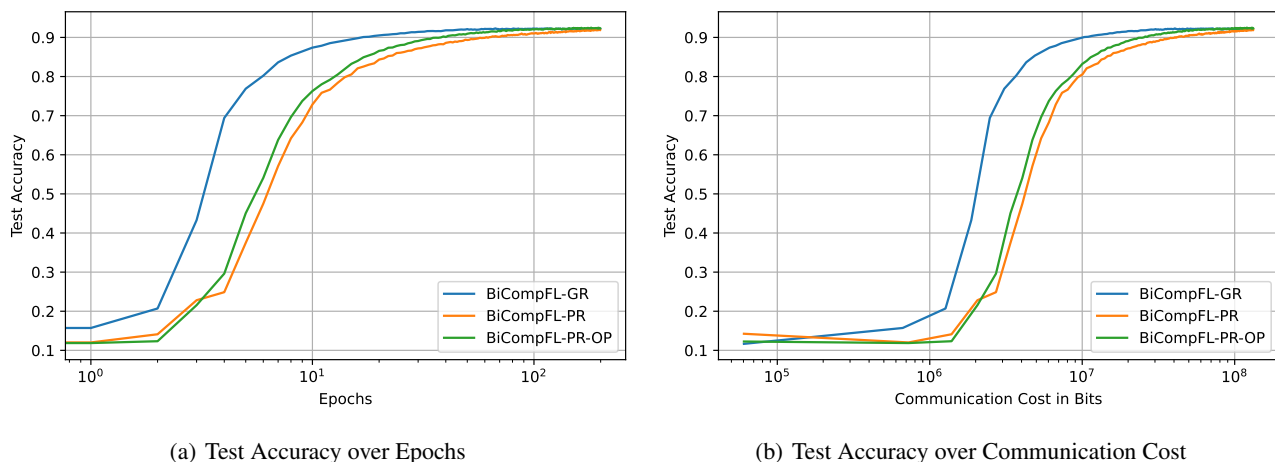


Figure 14: BiCompFL-PR With and Without Optimization over the Prior. Optimization over the Priors is denoted by OP.

It can be found that, while optimizing the prior improves the accuracy over epochs and with respect to the communication cost compared to BiCompFL-PR the improvements are rather insignificant. We therefore present for clarity the algorithm with a fixed choice of the prior as the former global model estimate, which additionally reduce the computation overhead at the clients by avoiding the optimization over λ . Nonetheless, we note that in certain edge cases, there can be merit in the optimization approach, for instance when the number n_{DL} of samples on the downlink is very small, and hence the global model estimate is inaccurate.

J.3 Number of Samples

We continue to assess the impact of the number n_{DL} of samples on the downlink. We therefore evaluate the performance of BiCompFL-PR for $n_{DL} \in \{5, 10, 20\}$. We evaluate the differences on BiCompFL-PR. The results in Fig. 15 reflect the obvious: the larger n_{DL} , the better the accuracy when plotted over the number of epochs. On the contrary, the larger n_{DL} , the larger the communication cost per epoch. The final accuracies do not show substantial differences, and hence, $n_{DL} = 5$ is sufficient in this setting. To avoid assessing our method overly optimistic and provide a fair comparison to other methods, we choose $n_{DL} = 10$ in all our experiments, noting that the communication can further be reduced in certain scenarios by lowering n_{DL} without notable performance loss.

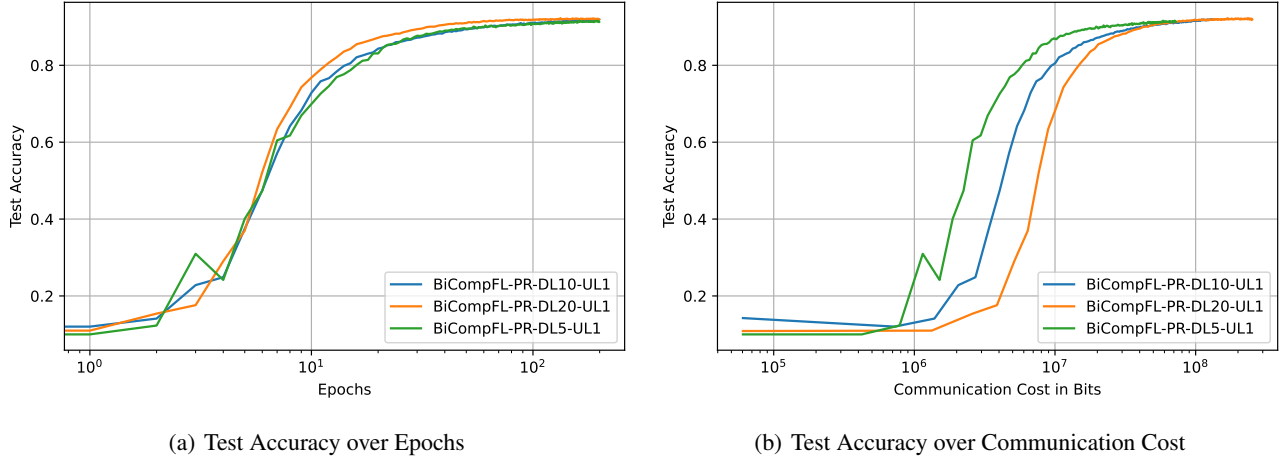


Figure 15: BiCompFL-PR for Different Number of Downlink Samples and a Single Uplink Sample.

J.4 Block Size

We compare in Fig. 16 the performance of BiCompFL-GR for different block sizes $BS = d/B \in \{128, 256, 512\}$. As expected, fixing n_{IS} , larger block sizes worsen the performance of the algorithm when evaluated over the number of epochs. However, larger block sizes simultaneously reduce the communication cost, and can hence be beneficial in many scenarios. However, we also note that larger block sizes comes at the expense of increases sampling complexities, and hence, the maximum block sizes are also dominated by the resources of the clients and the federator.

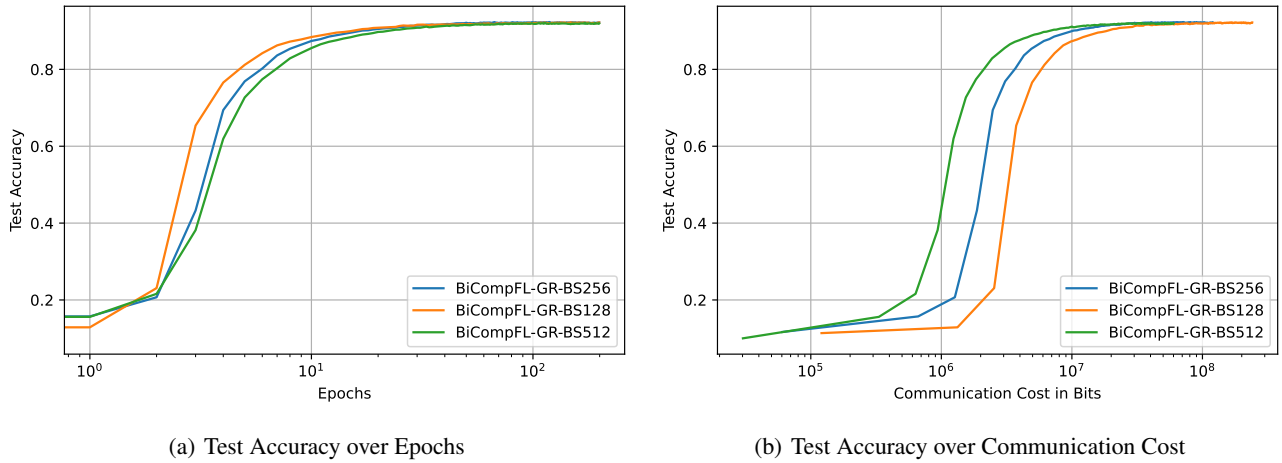
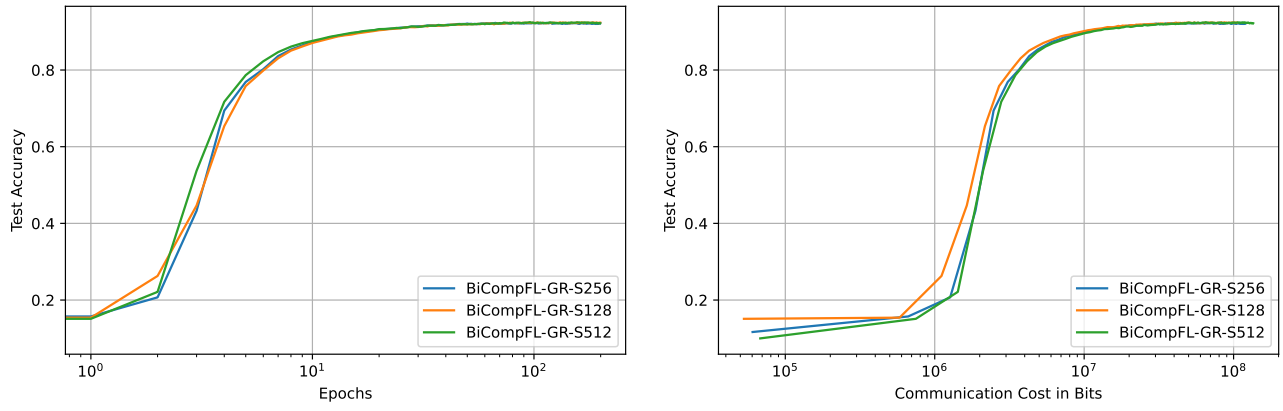


Figure 16: BiCompFL-GR With Fixed Block Allocation for Varying Block Sizes (BS) d/B .

J.5 Number of Importance Samples

In Fig. 17, we study the sensitivity of our algorithms with respect to the number of importance samples n_{IS} at the example of BiCompFL-GR. While larger number of n_{IS} slightly improves the performance as of the epoch number, the improvements do not outweigh the additional communication costs. Overall, our algorithm proves rather stable within reasonable ranges for n_{IS} . We fix in all our experiments $n_{IS} = 256$, presenti



(a) Test Accuracy over Epochs

(b) Test Accuracy over Communication Cost

Figure 17: BiCompFL-GR with Varying Number of Importance Samples n_{IS} per Block.